

Proceedings of the 15th International Newborn Brain Conference: Neuro-imaging studies

Fota Island, Cork, Ireland, February 28th – March 2nd 2024

AbdulAziz Al-Garni, Saima Aslam, Zarina Assis, Karman Avanski, Maria Chiara Bagnato, Alan Bainbridge, Kelly Pegoretti Baruteau, Renzo Beghini, Juliana Benavides, Amina Benlamri, Angelika Berger, Megan Ni Bhroin, Francesca Bissolo, Arun Bokde, Elena Bonafiglia, Martijn Boomsma, Martijn F. Boomsma, Vivianne Boswinkel, Geraldine Boylan, Julia Buchmayer, Joe Bwambale, Angela Byrne, Fady T. Charbel, Sara Cherkerzian, Gabrielle Collieran, Gabriel Cote-Corriveau, Frances Cowan, Anais Durand, Mohamed El-Dib, Hoda El-Shibiny, Alia Embaireeg, Carmina Erdei, Hugo A. Ferreira, Elsa Fiedrich, Carlo Alberto Forcellini, Rossella Frassoldati, Renate Fuiko, Renate Fuiko, Aisling Garvey, Juri G. Gelovani, Gilbert Gilbert, Katharina Goeral, Katharina Goeral, Ipsita Goswami, Patricia Ellen Grant, Laila Hadava, Mimily Harsono, Misa Hashimoto, Lena Hellström-Westas, Leonora Hendson, Emma Hofland-Burphy, Tim Hurley, Terrie Inder, Tarikul Islam, Yuji Ito, Camilo Jaimes, Raphaela JernejGregor Kasprian, Michael Kawooya, Lynne Kelly, Hiroyuki Kidokoro, Patric Kienast, Regan King, Sumire Kumai, Alexander Leemans, Lara M. Leijser, Marguerite Leoni, Jun Li, Samson K Lubowa, Takashi Maeda, Pradeep Mally, Ivan Mambule, Rayyan Manwar, Nuno Matela, Sean Mathieson, Avneet Mazara, Laura S. McGuire, Gerda Meijler, Martha G. Menchaca, H el ene Meunier, Takamasa Mitsumatsu, Khorshid Mohammed, Eleanor Molloy, Sarfaraz Momin, Nuno Canto Moreira, Jamiir Mugalu, Prashanth Murthy, Allena Nabawanuka, Tomohiko Nakata, Annetee Nakimuli, Carol Nanyunja, Hajime Narita, Nima Naseh, Jun Natsume, Chiara Nosarti, Tatiana Nuzum, Moffat Nyirenda, Mary O’Dea, Laura Pecoraro, Sofia Pellizzari, De-Ann M. Pillers, Massroor Pourcyrous, Divya Rana, Nicola Robertson, Sriya Roychaudhuri, Samantha Sadoo, Yoshiaki Sato, Fumi Sawamura, Jeanne Scotland, James Scott, Danielle Sharon, Anna Shiraki, Anthony Shoo, Amanda P. Siegel, Elizabeth Singh, Marie Slevin, Latha Srinivasan, Huzair Ssesembo, Nina Stein, Sophie Stummer, Ryosuke Suzui, Deirdre Sweetman, Eniko Szakmar, Gentaro Taga, Selphee Tang, Cally Tann, Chantal Tax, Francisco Torrealdea, Lucy Vanes, T ania F. Vaz, Sujith Gurram Venkata, Mariela Adriana Ventola, Anouk Verschuur, Elena Wachtel, Brian Walsh, Hama Watanabe, Emily Webb, Gerda van Wezel-Meijler, Pia Wintermark, Misae Yamada, Hiroyuki Yamamoto, Hussein Zein, Arianna Zuccato

Consensus brain injury classification predicts long-term outcomes in hypoxic ischemic encephalopathy infants after therapeutic hypothermia

Alia Embaireeg¹, Sarfaraz Momin¹, Prashanth Murthy¹, Amina Benlamri^{1,3}, Elsa Fiedrich^{1,3}, Lara Leijser¹, Hussein Zein¹, James Scott², Zarina Assis², Sujith Gurram Venkata¹, Selphee Tang³, Jun Li⁴, Khorshid Mohammad¹

¹Department of Pediatrics, Section of Neonatology, University of Calgary, ²Department of Diagnostic Imaging, Division of Neuroradiology, University of Calgary, ³Department of Pediatrics, Neonatal Follow - Up Clinic, Alberta Children’s Hospital, University of Calgary, ⁴Cumming School of Medicine, University of Calgary

BACKGROUND: Hypoxic Ischemic Encephalopathy (HIE) is a significant cause of perinatal encephalopathy, affecting a substantial number of neonates. Therapeutic hypothermia (TH) has become a standard treatment, significantly reducing mortality leaving a portion of survivors with varying degrees of neurodevelopmental impairment. Neuroimaging, specifically magnetic resonance imaging (MRI), plays a crucial role in prognostication. A standardized MRI scoring system to assess brain injury severity and extent is crucial for predicting long term neurodevelopmental outcome.

OBJECTIVES: This study aimed to investigate the predictive value of the Canadian Standardized consensus classification of brain injury diagnosed with MRI on long – term neurodevelopmental outcomes at 18 – 24 months of corrected age in infants with HIE post therapeutic hypothermia.

Table 3a: MRI scores and death or any NDI excluding ASQ results at 21 months (death, uncontrolled seizure disorder, CP, vision or hearing impairment, or any Bayley score <85)

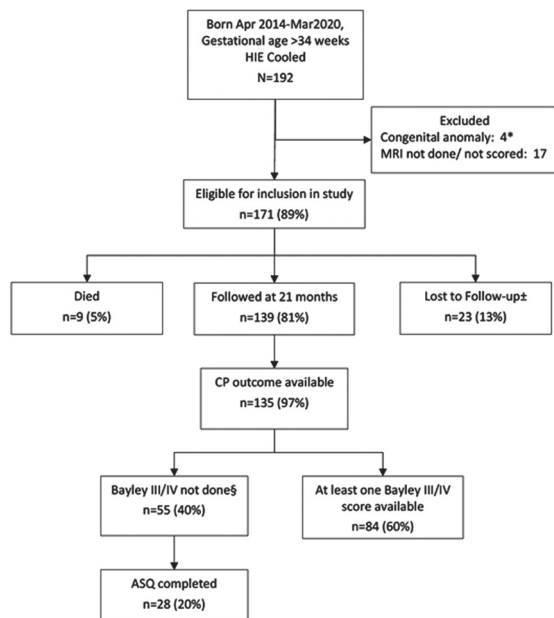
	No death or adverse outcome (n=29)	Death or adverse outcome (n=46)	p-value*
Grey Matter excl. 1H-MRS, median (IQR)	0 (0-0)	3 (0-11)	<0.001
Grey Matter incl. 1H-MRS, median (IQR)	0 (0-0)	3 (0-12)	<0.001
White Matter, median (IQR)	0 (0-0)	3.5 (0-11)	<0.001
Cerebellum, median (IQR)	0 (0-0)	0 (0-0)	0.106
Additional, median (IQR)	0 (0-1)	0 (0-1)	0.871
MRI Total Score excl. 1H-MRS, median (IQR)	0 (0-1)	6.5 (1-19)	<0.001
MRI Total Score incl. 1H-MRS, median (IQR)	0 (0-1)	6.5 (4-21)	<0.001

*Mann-Whitney U test.

Table 3b: MRI scores and death or any NDI including ASQ results at 21 months (death, uncontrolled seizure disorder, CP, vision or hearing impairment, or any Bayley score <85, or if Bayley not done, any ASQ score below the cut-off)

	No death or adverse outcome (n=43)	Death or adverse outcome (n=56)	p-value*
Grey Matter excl. 1H-MRS, median (IQR)	0 (0-0)	0 (0-9)	<0.001
Grey Matter incl. 1H-MRS, median (IQR)	0 (0-1)	1 (0-9)	<0.001
White Matter, median (IQR)	0 (0-0)	3 (0-10)	<0.001
Cerebellum, median (IQR)	0 (0-0)	0 (0-0)	0.066
Additional, median (IQR)	0 (0-1)	0 (0-1)	0.923
MRI Total Score excl. 1H-MRS, median (IQR)	0 (0-2)	5 (1-18)	<0.001
MRI Total Score incl. 1H-MRS, median (IQR)	1 (0-2)	5.5 (1-19)	<0.001

*Mann-Whitney U test.



*Excluded n=1 with polymicrogyria and chromosomal microdeletion, n=1 with tracheoesophageal fistula, n=1 with congenital hip dysplasia, and n=1 with THRA gene variant.
 ±Babies not seen at 21 months or nursing-only phone assessments at 21 months were considered lost-to-follow-up. Babies not seen at 21 months but nursing phone assessments indicated uncontrolled seizure disorder and severe delays were included.
 §Babies born from approximately 2018 June to 2019 October could not be administered the Bayley due to pandemic restrictions, however data from virtual or in-person physician visits and ASQ questionnaire results may have been available.

Table 1: Baseline characteristics and MRI scores

Characteristic	Died or followed at 21 months N=148
Gestational age (wks), mean (SD), range	39 (2) Range 35-42
Birth weight (g), mean (SD), range	3347 (581) Range 2090-4700
Male, n (%)	90 (61%)
Appgar at 1 minute, median (IQR), range	1 (1-3) Range 0-9 (missing=1)
Appgar at 5 minutes, median (IQR), range	4 (3-6) Range 0-9 (missing=1)
Appgar at 10 minutes, median (IQR), range	6 (4-7) Range 0-9 (missing=11)
Age at MRI (day of life), median (IQR), range	4 (4-4) Range 0-29
Grey Matter excl. 1H-MRS, median (IQR), range	0 (0-2) Range 0-23
Grey Matter incl. 1H-MRS, median (IQR), range	0 (0-3) Range 0-25
White Matter, median (IQR), range	0 (0-4) Range 0-15
Cerebellum, median (IQR), range	0 (0-0) Range 0-4
Additional, median (IQR), range	0 (0-1) Range 0-2
MRI Total Score excl. 1H-MRS, median (IQR), range	2 (0-7) Range 0-36
MRI Total Score incl. 1H-MRS, median (IQR), range	2 (1-8) Range 0-38

Table 2: Outcomes at 21 months (actual age at visit ranges between 17 and 28 months)

	Died or followed at 21 months N=148
Death, n (%)	9 (6.1%)
Uncontrolled seizure disorder	4/135 (3.0%)
Cerebral Palsy, n (%)	
No CP	125/135 (92.6%)
CP GMFCS 1-2	6/135 (4.4%)
CP GMFCS 3-5	4/135 (3.0%)
Vision§	
No impairment	122/126 (96.8%)
Significant impairment	2/126 (1.6%)
Bilateral blindness	2/126 (1.6%)
Hearing†	
No neurosensory loss	124/126 (98.4%)
Mild-moderate neurosensory loss	1/126 (0.8%)
Bilateral deafness	1/126 (0.8%)
Bayley Scores* <85, n (%)	
Cognitive	14/82 (17.1%)
Language	12/56 (21.4%)
Motor	12/62 (19.4%)
Any of cognitive, language, motor	28/60 (46.7%)
Any Bayley score <85, or if Bayley not done, any ASQ score below the cut-off‡	38/88 (43.2%)
Death, uncontrolled seizure disorder, CP, vision or hearing impairment, or any Bayley score <85	46/75 (61.3%)
Death, uncontrolled seizure disorder, CP, vision or hearing impairment, or any Bayley score <85, or if Bayley not done, any ASQ score below the cut-off	56/99 (56.6%)
Any NDI (uncontrolled seizure disorder, CP, vision or hearing impairment, or any Bayley score <85)	37/66 (56.1%)
Severe NDI (uncontrolled seizure disorder, CP GMFCS 3-5, bilateral blindness, bilateral deafness, or any Bayley score <70)	17/59 (28.8%)

* Bayley III except for n=3 children who were assessed using the Bayley IV.
 ‡ Any of ASQ communication, gross motor, fine motor, problem solving, or personal-social scores categorized as "below the cut-off".
 § Significant visual impairment defined as one or more of: corrected visual acuity <20/60 and >20/200 but not bilaterally blind; unilateral blindness; nystagmus; registered with CNIB but not legally blind; bilateral blindness defined as one or more of: corrected visual acuity <20/200 in the better eye, light perception or less in the better eye, cortical blindness or atrophy, legally blind.
 † Mild-moderate neurosensory hearing loss defined as any neurosensory hearing loss not requiring amplification/cochlear implants or unilateral deafness requiring amplification; bilateral deafness defined as bilateral neurosensory hearing loss or auditory neuropathy requiring amplification/cochlear implants.

METHODS: A Retrospective observational cohort study conducted between April 2014 and March 2020 included term and near – term neonates with moderate to severe HIE who underwent TH and had MRI imaging to evaluate brain injury who were admitted to a tertiary care center in Calgary, Alberta. Institutional criteria for TH eligibility were defined. A Canadian consensus scoring system, categorizing various patterns of brain injury, was applied to the MRI scans. Follow up at 18 – 24 months adjusted age assessed neurodevelopmental outcomes. The data was compiled and underwent statistical analysis using SAS software, Version 9.4. Tests used were two sided and significance defined as a p-value <0.05

RESULTS: Of the 171 infants included, 5% died and 81% were assessed for neurodevelopmental outcomes. Among surviving infants, a substantial proportion exhibited various degrees of neurodevelopmental impairment, including severe NDI (28.8%), any NDI (56.1%), severe cerebral palsy (3%) and uncontrolled seizure disorder (3%). Lower composite Bayley scores were observed in 46.7% of infants. MRI scores were associated with these outcomes, underscoring the utility of the MRI scoring system for predicting adverse neurodevelopmental outcomes.

CONCLUSION: This study demonstrates the significant long – term consequences of moderate to severe HIE, even after therapeutic hypothermia. The standardized Canadian consensus MRI classification offers a valuable tool for predicting these outcomes and can guide treatment

decisions and support families. Further research and validation of these findings are necessary to enhance care and management for infants with neonatal encephalopathy, providing improved prognostication and potentially better long term outcomes.

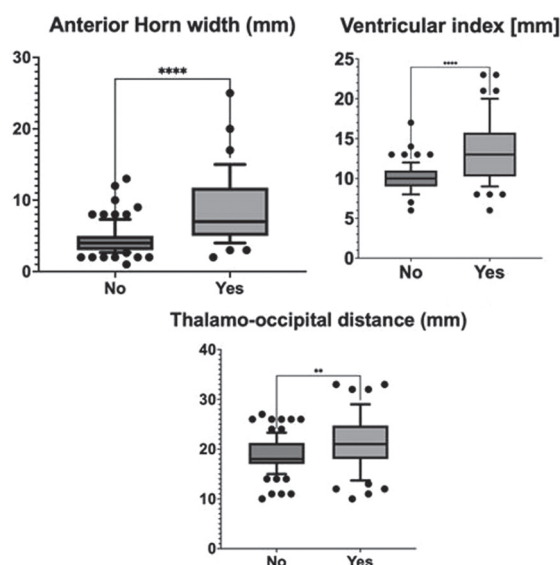
Integrating clinical and neuroimaging markers to predict onset of post-hemorrhagic ventricular dilatation in preterm neonates

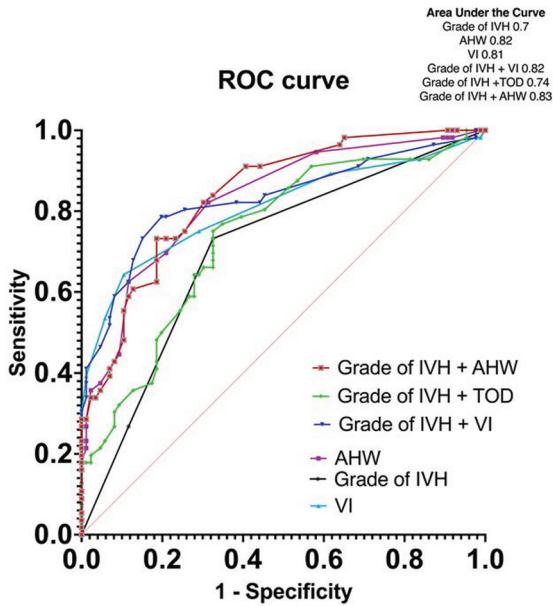
AbdulAziz Al-Garni¹, Avneet Mazara¹, Nina Stein^{1,2}, **Ipsita Goswami^{1,2}**

¹McMaster Children’s Hospital, ²Hamilton Health Sciences

BACKGROUND AND OBJECTIVE: Posthemorrhagic ventricular dilatation (PHVD) is one of the major complications of intraventricular hemorrhage (IVH) and accounts for almost 30-40% of infants with Grade 2-4 IVH. PHVD is associated with higher risk of death or developmental impairment such as cerebral palsy, cognitive, functional, and attention deficits compared to infants with IVH without ventricular dilatation. All preterm infants with IVH are diagnosed within a week of life and subsequent serial ultrasounds (US) are needed to detect the infants who develop PHVD. This study aims to explore the early perinatal risk factors in addition to the Grade of IVH associated with the progression to PHVD, with the ultimate goal of developing a predictive model using key clinical and neuroimaging-based predictors.

METHODOLOGY: A retrospective chart review of preterm infants ≤29 weeks gestational age (GA) and



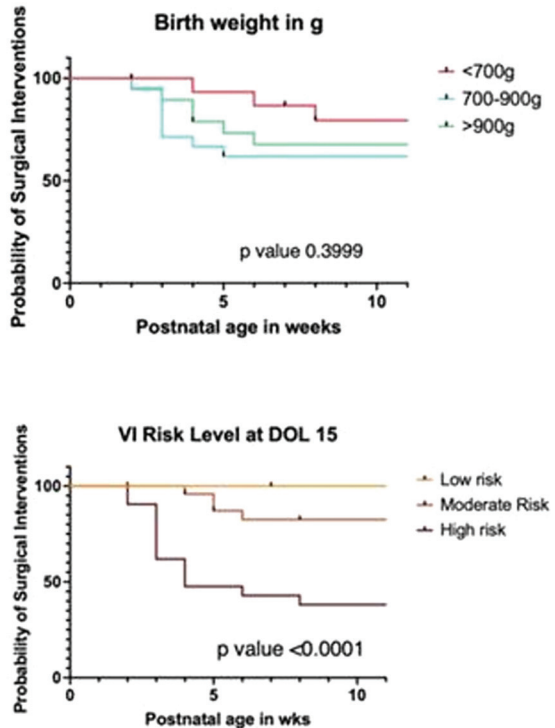
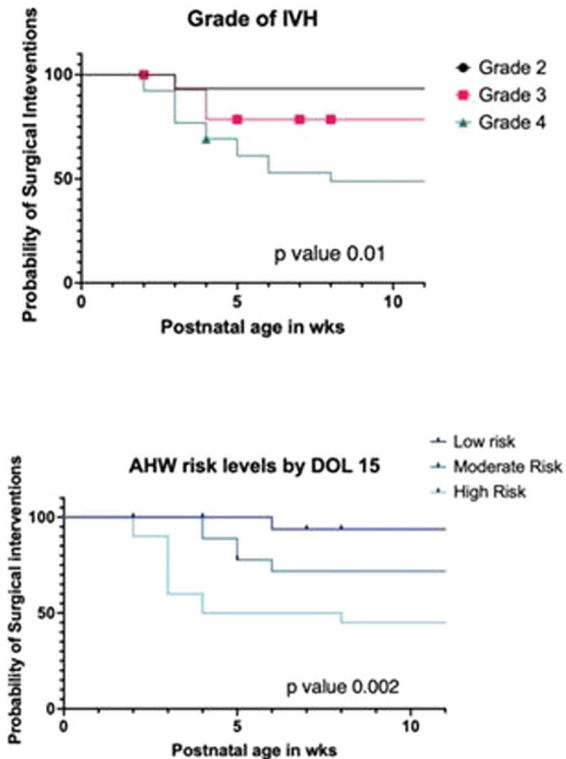


birthweight (BW) ≤ 1500 g with Grade 2,3,4 IVH, admitted between January 2015-December 2021 were included. All cranial US done within 2weeks postnatal age were assessed for Grade of IVH, Anterior Horn Width (AHW), Ventricular Index (VI) and Thalamooccipital Index (TOD) according to the Canadian consensus statement. Only the highest grade and dimension on either side were considered

for data analysis. Primary composite Outcome was defined as death or any US with VI or AHW or TOD \geq moderate risk based on Eldib et al[1] between 2weeks postnatal age or 40 weeks postmenstrual age.

RESULTS: A total of 146 infants with a mean (SD) GA of 26 (1.8) weeks, BW 900 (234)g and female (46%) were included (excluded 4 for missing data). The primary outcome occurred in 56 (39%), ventricular reservoir was needed in 17 (30%) and Shunt insertion was needed in 11 (20%). The clinical characteristics of infants with and without the composite outcome were comparable except that the former were significantly smaller and received >2 doses of surfactant [Table 1]. On multivariate logistic regression, the risk factors present within 2 weeks postnatal age that significantly increased the odds of developing PHVD were hemodynamically significant duct arteriosus [OR 6.1 (95%CI 1.9-22)], culture-proven sepsis [OR 5.4 (95%CI 1.8-18)], Grade 3 IVH [OR 4.6 (95%CI 1.1-22)], Grade 4 IVH [OR 3 (95%CI 0.9-10)], and VI(mm)[OR 2.1 (95%CI 1.6-2.9)] [Table 2, Figure 1]. On survival analysis, surgical interventions were noted to be done at earlier postnatal age in neonates whose VI and AHW were at high-risk levels by 2weeks postnatal age and those with Grade 4 IVH [Figure 2].

CONCLUSION: In addition to the Grade of IVH, clinical predictors such as hemodynamically significant duct arteriosus and bacterial septicemia along with risk levels



of US-based markers such as AHW and VI measured within 2 weeks of life are potential predictors of later onset of PHVD. Validity of the proposed predictor model will need to be tested in a larger cohort.

BIBLIOGRAPHY

1. El-Dib M et al. J Pediatr. 2020 Nov;226:16-27.e3

Cerebellar pathologies in extremely preterm infants with intraventricular hemorrhage in relation to neurodevelopmental outcome

Julia Buchmayer¹, Gregor Kasprian², Sophie Stummer¹, Renate Fuiko¹, Patric Kienast², Angelika Berger¹, Katharina Goeral¹

¹Comprehensive Center for Pediatrics, Department of Pediatrics and Adolescent Medicine, Division of Neonatology, Intensive Care and Neuropediatrics, Medical University of Vienna, ²Department of Radiology, Division of Neuroradiology and Musculoskeletal Radiology, Medical University of Vienna

OBJECTIVES: Extremely preterm birth and intraventricular hemorrhage (IVH) are established risk factors for adverse neurodevelopmental outcome. As IVH is often associated with cerebellar hemorrhage (CBH), the additional influence on development of these posterior fossa abnormalities is warranted.

METHODS: This observational cohort study analyzed cerebral magnetic resonance imaging data at term-equivalent age of patients <28 weeks of gestation with IVH born between 2011 and 2021 at the level IV Neonatal Intensive Care Unit of the Medical University of Vienna. Cerebellar hemorrhage was graded according to Kidokoro et al(1) as shown in Figure 1, with grade I consisting of unilateral punctate lesions ≤3 mm in size, grade II consisting of bilateral punctate lesions ≤3 mm, grade III consisting of a unilateral lesion >3 mm and grade IV was diagnosed when extensive lesions were observed bilaterally. In addition, a category of “cerebellar atrophy” was introduced, including atrophy of at least one third of one hemisphere due to hemorrhage or intracranial pressure (e.g. trapped fourth ventricle). Additionally, cerebellar growth was categorized by measurement of transverse cerebellar diameter. Finally, the impact of injuries on outcome at two-years corrected age (tested with

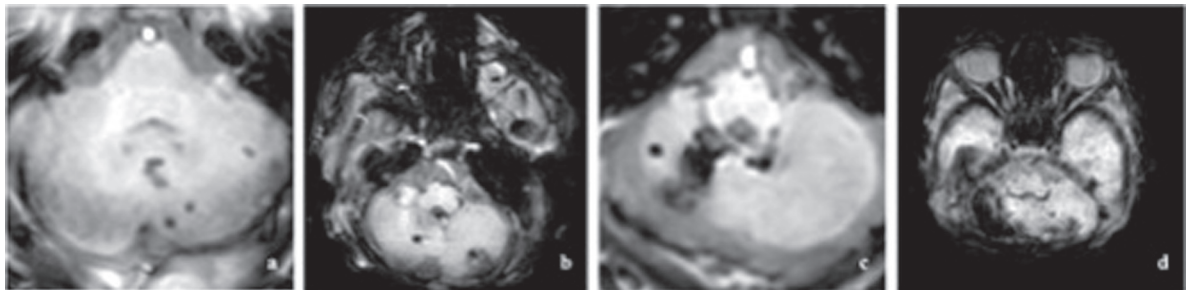


Figure 1. Classification of cerebellar hemorrhage, with a unilateral punctate lesions (≤3 mm); b bilateral punctate lesions (≤3 mm); c unilateral extensive hemorrhage (>3 mm); d bilateral extensive hemorrhage (>3 mm).

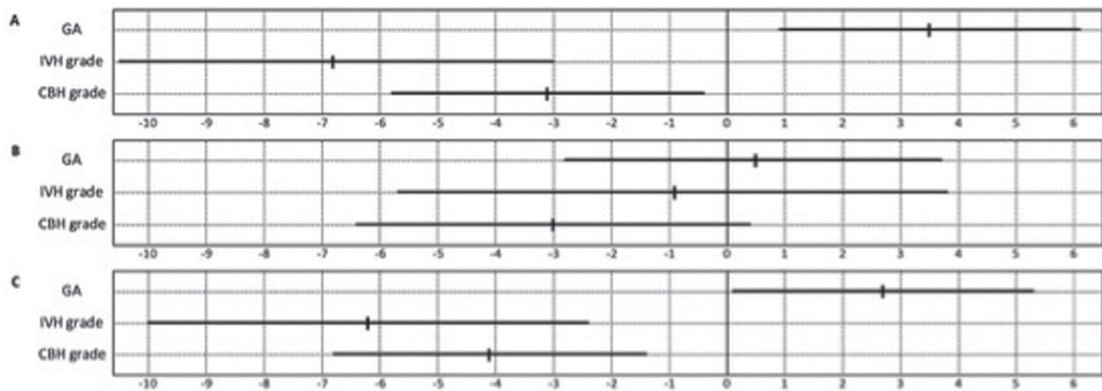


Figure 2. Forest plot representing unstandardized coefficients (B) along with their 95% confidence intervals of predictor variables on A cognitive, B language and C motor outcome calculated using multivariable regression analysis.

Bayley-III) was evaluated, incorporating multivariable regression analysis.

RESULTS: Among 103 patients, 69 (67%) showed CBH with a median grade of 1 (IQR 0-3). At two-years corrected age CBH was significantly associated with impaired cognitive and motor outcome. Also, multivariable regression models identified CBH as an independent predictor of poor cognitive, language and motor development at two-years corrected age, as shown in Figure 2. Cerebellar atrophy, affecting 30 (29%) infants, was linked to significantly impaired outcome across all domains (cognitive, language and motor). Conversely, increasing cerebellar size correlated with better motor development ($p=0.04$).

CONCLUSION: Extremely preterm infants with IVH and concomitant CBH showed significant cognitive and motor impairment. The extent of CBH was associated with the grade of developmental delay, mainly regarding motor development. These findings may support prediction of long-term outcome and parental counseling in patients with IVH.

REFERENCE:

(1) Kidokoro H, Anderson PJ, Doyle LW, Woodward LJ, Neil JJ, Inder TE. Brain injury and altered brain growth in preterm infants: predictors and prognosis. *Pediatrics*. Aug 2014;134(2):e444-53. doi:10.1542/peds.2013-2336

Early versus late brain magnetic resonance imaging and spectroscopy in infants with neonatal encephalopathy

Tatiana Nuzum, Pradeep Mally, Elena Wachtel

¹Hassenfeld Children's Hospital at NYU Langone, ²NYCH+H Bellevue Hospital Center

BACKGROUND: Magnetic Resonance (MR) Imaging is the current gold standard for early neurodevelopmental prognostication of infants with Neonatal Encephalopathy (NE). Recent studies have suggested that obtaining MR imaging (MRI) at a single time-point may underestimate the degree of neurologic injury. MR Spectroscopy (MRS) is a newer modality of neuroimaging that may be more sensitive in the detection of hypoxic-ischemic injury.

OBJECTIVE: To evaluate the utility of early and late MRI in infants with NE, and to determine the concordance between MRS and initial MRI.

METHODS: This was a retrospective chart review including infants with NE born between 2017 and 2023 at two regional perinatal centers, NYU Langone Health and Bellevue Hospital Centers. Demographic and clinical

Variable	Subjects (n = 98)
Gestational Age (weeks)*	38.97 ± 1.65
Birth Weight (g)*	3201.89 ± 549.28
Female Sex*	39 (39.8%)
Delivery via Cesarean Section*	65 (66.3%)
Outborn*	64 (65.3%)
Apgar Score – 1 minute [‡]	2 [1, 2]
Apgar Score – 5 minutes [‡]	4 [3, 6]
Apgar Score – 10 minutes [‡]	6 [4, 7]
Apgar Score – 15 minutes [‡]	6 [4, 7]
Resuscitative Measures in Delivery Room*	
Intubation	65 (66.3%)
Chest Compressions	19 (19.4%)
Epinephrine	14 (14.3%)
Venous Cord Gas pH*	7.10 ± 0.21
Venous Cord Gas Base Deficit*	11.89 ± 6.07
Arterial Cord Gas pH*	6.99 ± 0.16
Arterial Cord Gas Base Deficit*	14.08 ± 7.01
Postnatal Gas pH*	7.11 ± 0.16
Postnatal Gas Base Deficit*	16.96 ± 5.83
Postnatal Lactate*	12.21 ± 4.41
Sarnat Grade of Encephalopathy*	
Mild	9 (9.2%)
Moderate	76 (77.5%)
Severe	13 (13.3%)
Abnormality of video electroencephalogram*	
Mild	39 (40.2%)
Moderate	22 (22.7%)
Severe	36 (37.1%)

* = mean ± *sd*, † = n (%), ‡ = median [IQR]

information including MRI results were collected. All infants underwent early diffusion-weighted MRI with MRS, and late conventional T1/T2-weighted imaging.

RESULTS: Ninety-eight infants were included. Subject demographics are described in Table 1. The majority (78%) were moderately encephalopathic. Early and late MR imaging was performed at an average of 5.7 and 13.6 days of life respectively. Both MRIs were assigned an injury severity score based on the NICHD NRN pattern of injury. Differences in these scores between first and second MRIs are outlined in Table 2. Forty percent of infants exhibited a change in severity of injury between early and late MRI. Twenty-three infants (24%) were found to have milder injury and 16 (16%) were found to have more severe injury according to late imaging. Fifteen percent of infants had evidence of hypoxic-ischemic injury on early imaging only, and 6% on late imaging only. Eighty infants (82%) underwent MRS with early imaging. Concordance of injury severity between MRS and MRI was 62.5%. Among the cases of discordant MRI/MRS, MRS detected additional injury in 70% of cases, and MRI detected additional injury in 30% of cases. MRI findings unrelated to hypoxic-ischemic injury are also outlined in Table 2.

CONCLUSION: Both early and late imaging are necessary to fully define neurologic injury and provide accurate neurodevelopmental prognoses in cases of neonatal encephalopathy. Had imaging not been performed at two intervals, radiologic diagnoses of hypoxic-ischemic

	First MRI (n = 98)	Second MRI (n = 98)
Age (days) at time of imaging*	5.68 ± 1.44	13.63 ± 4.28
MRS performed*	80 (81.6%)	
MRI/MRS Concordance*	50 (62.5%)	
MRS detected injury not seen on MRI	21 (70%)	
MRI detected injury not seen on MRS	9 (30%)	
NICHD Score based on Diffusion-Weighted and T1/T2-weighted imaging*		
0	50 (51.0%)	62 (63.3%)
1A/1B	19 (19.4%)	11 (11.2%)
2A/2B	28 (28.6%)	21 (21.4%)
3	1 (1.0%)	4 (4.1%)
Non HIE-related findings*		
Sub-arachnoid Hemorrhage	5 (5.1%)	4 (4.1%)
Intraventricular Hemorrhage	6 (6.1%)	3 (3.1%)
Parenchymal Hemorrhage	10 (10.2%)	5 (5.1%)
Other Incidental Findings	4 (4.1%)	5 (5.1%)
Early vs. Late Imaging		
Change in NICHD Score on late imaging*	39 (39.8%)	
Decrease in Score/Severity*	23 (23.5%)	
Increase in Score/Severity*	16 (16.3%)	
HIE apparent on first MRI only*	15 (15.3%)	
HIE apparent on second MRI only*	6 (6.1%)	

* = mean ± sd, * = n (%)

MRI = Magnetic Resonance Imaging, MRS = Magnetic Resonance Spectroscopy, NICHD = National Institute of Child Health and Human Development, HIE = hypoxic-ischemic encephalopathy.

injury would have been missed in 6-15% of cases, and characterization of injury may have been inaccurate in up to 40% of cases. Further analysis of MRS results with an independent reviewer may test the superiority of this modality in comparison to conventional MR imaging, given the discrepancy found in this study.

Methodological considerations on diffusion MRI tractography in infants aged 0-2 years: A scoping review

Anouk Verschuur^{1,2,3}, Regan King², Chantal Tax^{3,4}, Martijn Boomsma¹, Gerda van Wezel-Meijler¹, Alexander Leemans³, **Lara Leijser²**

¹Isala Hospital, ²University of Calgary, ³University Medical Center Utrecht, ⁴Cardiff University

OBJECTIVE: Understanding the intricate processes of typical and atypical brain development holds significant clinical importance, as many neurological and neurobehavioral disorders have their origins in the preterm period [1]. Diffusion magnetic resonance imaging (dMRI) tractography is a dedicated method to study the micro-structural architecture of the brain’s white matter [2]. Despite a keen interest to increase the understanding of the

rapidly developing young brain through tractography, detailed descriptions on how to approach tractography in infants are limited. The purposes of this review were 1) to describe current tractography methods as used on young infant dMRI data and summarize their limitations, and 2) to provide recommendations for advanced tractography in young infant brains.

METHODS: Through a scoping review, methodological approaches to white matter tractography and their commonly reported limitations in infants aged 0-2 years are evaluated. A search was performed in July 2022.

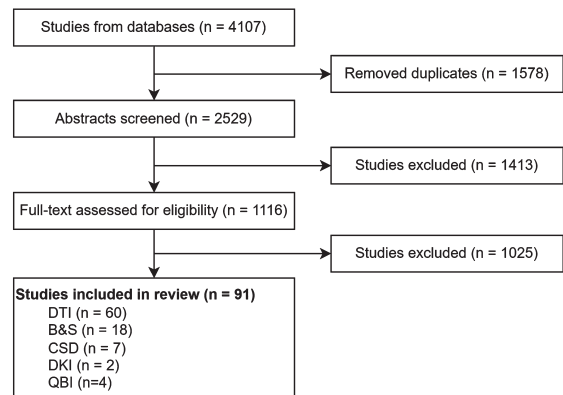


Figure 1: In/exclusion flowchart of identified and eligible papers on diffusion MRI tractography in the infant (0-2 years of age) brain.

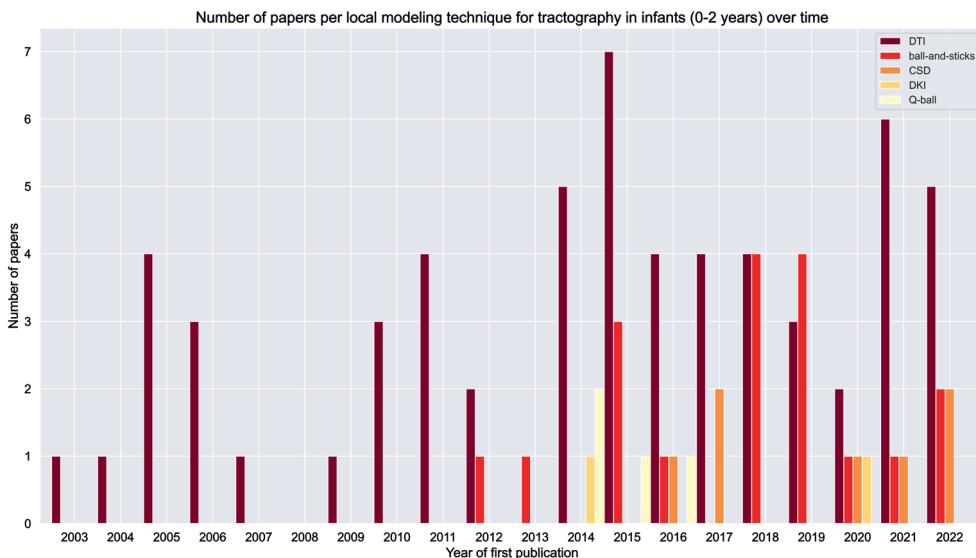


Figure 2: Progression of used methods for infant brain tractography over time.

Studies applying white matter tractography on brain scans of infants who underwent dMRI between birth and two years of age were included. Papers that described tractography on a single fiber bundle, single scan, or for whole brain connectome analysis were excluded. Ongoing research, studies with missing details on tractography, and re-use of tractography data were also excluded. Screening of papers was performed independently by two researchers and discussed in a consensus meeting. A third researcher was consulted if consensus could not be reached.

RESULTS: A total of 2529 papers were identified, of which 1413 were excluded based on title and abstract. An additional 1025 papers were excluded after full text screening (Figure 1). The 91 remaining papers were

considered eligible for this review. The majority (66%) of included tractography literature described the use of diffusion tensor imaging (DTI; Figure 2) [2]. Despite having the potential for more detailed reconstruction of the organizationally complex white matter, especially in crossing nerve bundles, and extensive knowledge gained from application on the adult brain. Only few studies described advanced tractography approaches, including constrained spherical deconvolution (CSD; Figure 3), diffusion kurtosis imaging (DKI), ball-and-sticks model (B&S) and Q-ball imaging (QBI) [3-7]. This may be partly attributed to technical challenges with imaging, image processing and the need for short scan times in young children.

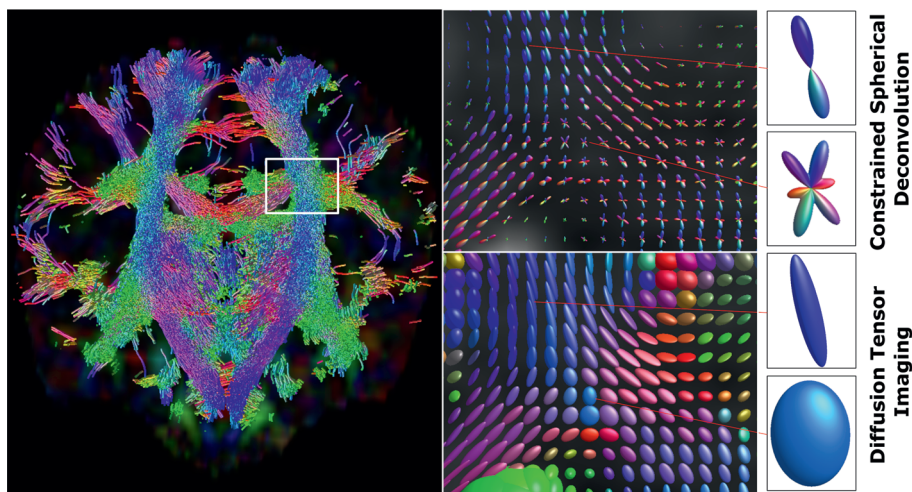


Figure 3: Constrained spherical deconvolution (CSD) versus diffusion tensor imaging (DTI) in the centrum semiovale where the corpus callosum and corticospinal tracts cross. In contrast to DTI, CSD allows for reconstruction of multiple fiber orientations in a single voxel, enabling reconstruction of crossing fiber bundles.

CONCLUSION: Optimization of the largely unexplored advanced tractography approaches for use in young infants is warranted. More reliable reconstruction of the developing and vulnerable white matter contributes to distinguishing subtle differences between typical and atypical brain development, and may contribute to early recognition, personalized treatment plans and improved prognosis and monitoring of developmental disorders in young infants.

Evaluation of brain extraction techniques in preterm neonatal MRI at term: implications for intracranial volumes

Tânia F. Vaz¹, Nuno Canto Moreira², Lena Hellström-Westas³, Nima Naseh³, Nuno Matela¹, Hugo A. Ferreira¹

¹Instituto De Biofísica E Engenharia Biomédica, Faculdade De Ciências Da Universidade De Lisboa, Portugal, ²Department of Neuroradiology, Karolinska University Hospital, ³Department of Women’s and Children’s Health, Uppsala University

BACKGROUND AND OBJECTIVE: Magnetic resonance imaging (MRI) plays a crucial role in evaluating early brain development and injuries in newborns [1]. For automated volumetric analysis, brain tissue segmentation is necessary, which requires brain extraction (BE) to exclude non-brain tissues. However, BE is challenging in neonatal brain MRI due to lower spatial resolution, lower signal-to-noise ratio, lower contrast-to-noise ratio, greater intensity variation within tissues, smaller brain size, evolving shape, and motion artifacts compared to adult brain images [2]. While various methods exist for BE, manual segmentation remains the standard approach. This study aims to evaluate different BE methods in preterm neonatal MRI and their impact on intracranial volumes (ICVs) at term-equivalent age (TEA).

METHODOLOGY: The study involved twenty-two premature neonates (mean gestational age ± standard deviation: 28.4±2.1 weeks) with brain MRI performed at TEA, without detectable lesions or congenital conditions. Manual segmentation of ICVs was performed using 3DSlicer on 2D T2-weighted scans to establish reference brain masks. Additionally, four automated BE methods were employed: HD Brain Extraction Tool (HD-BET) [3], Simple Watershed Scalping (SWS) [4], SynthStrip [5], and Brain Extraction Tool (BET2) [6]. Comparisons between BE methods were performed using voxel overlap-based and surface distance-based metrics. The Friedman’s test was used to assess significant differences, followed by post hoc tests corrected for multiple comparisons (Bonferroni-adjusted). Agreement between ICVs was reported using Bland-Altman analysis and volume-based metrics, whilst statistical analyses were conducted using IBM®SPSS® v27 software with a significance level of 5%.

RESULTS: The automated segmentations most similar to the manual segmentation were observed with the HD-BET and SWS, followed by the SynthStrip and BET2 methods (Table 1, Figure 1). Additionally, the root mean square error and respective coefficients of variation were: 13.8 mL (3.0%) for HD-BET, 10.5 mL (2.3%) for SWS, 13.6 mL (2.9%) for SynthStrip, and 33.8 mL (7.3%) for BET2.

CONCLUSION: HD-BET and SWS are the most similar to the manual segmentation, showing estimated ICVs with clinically-acceptable errors <3%.

BIBLIOGRAPHY:

- [1] Volpe JJ. Neurology of the Newborn. 5th ed. Saunders; 2008. p. 172-177.
- [2] Devi CN, Chandrasekharan A, Sundararaman VK, Alex ZC. Neonatal brain MRI segmentation: A review. Comput Biol Med. 2015;64:163–78.
- [3] Isensee F, Schell M, Pflueger I, Brugnara G, Bonekamp D, Neuberger U, et al. Automated brain extraction of multisequence MRI using artificial neural networks. Hum Brain Mapp. 2019;40(17):4952–64.

Table 1. Segmentation metrics statistics (median and interquartile range (IQR)) of four automated BE methods (HD-BET, SWS, SynthStrip, BET2).

	Median (IQR) of voxel overlap-based metrics							Median (IQR) of surface distance-based metrics (in mm)				
	Dice Coefficient	Jaccard Coefficient	Precision	Sensitivity	Specificity	False Positive Rate	False Negative Rate	Hausdorff Distance	Hausdorff Distance 95% Percentile	Mean Surface Distance	Median Surface Distance	Std. Deviation Surface Distance
HD-BET	0.968 [0.965,0.971]	0.938 [0.932,0.944]	0.958 [0.948,0.962]	0.983 [0.974,0.987]	0.995 [0.994,0.996]	0.005 [0.004,0.006]	0.017 [0.013,0.026]	7.200 [6.063,8.975]	3.156 [2.500,3.600]	0.596 [0.463,0.653]	0.000 [0.000,0.00]	1.008 [0.863,1.142]
SWS	0.966 [0.963,0.969]	0.934 [0.929,0.939]	0.977 [0.961,0.981]	0.959 [0.954,0.962]	0.998 [0.996,0.998]	0.003 [0.002,0.005]	0.041 [0.038,0.046]	27.339 [11.027,33.370]	3.600 [3.125,3.600]	0.651 [0.571,0.794]	0.000 [0.000,0.00]	1.471 [1.106,1.837]
SynthStrip	0.957 [0.952,0.961]	0.917 [0.909,0.925]	0.958 [0.944,0.964]	0.961 [0.947,0.969]	0.996 [0.994,0.996]	0.005 [0.004,0.006]	0.039 [0.031,0.053]	7.500 [7.218,9.674]	3.600 [3.125,3.600]	0.720 [0.654,0.941]	0.000 [0.000,0.00]	1.127 [1.032,1.281]
BET2	0.937 [0.933,0.941]	0.881 [0.874,0.889]	0.906 [0.896,0.912]	0.971 [0.959,0.980]	0.989 [0.988,0.990]	0.011 [0.010,0.012]	0.029 [0.020,0.041]	32.357 [31.318,33.586]	3.600 [3.600,4.438]	1.382 [1.282,1.582]	0.884 [0.625,0.975]	1.940 [1.748,2.166]

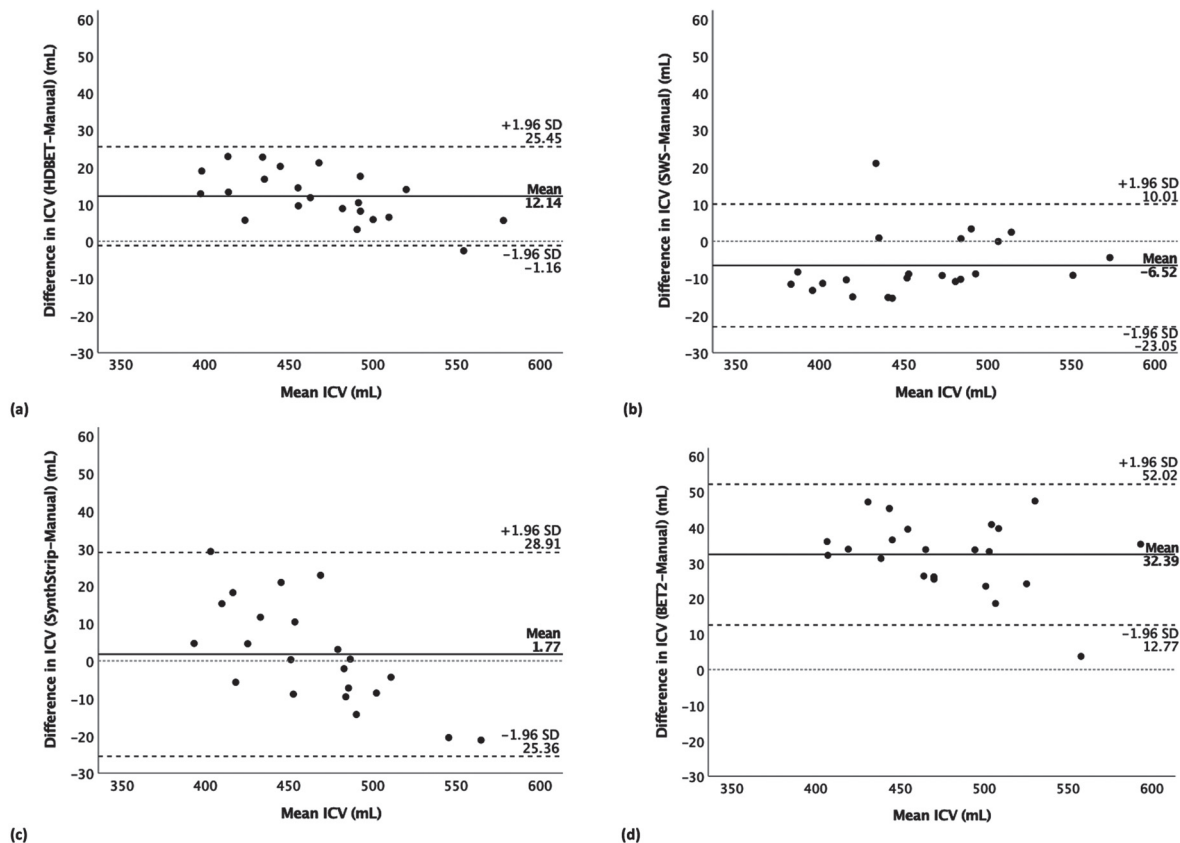


Figure 1. Bland-Altman analysis of the mean of ICV (X-axis) and the difference between (Y-axis) the automated BE methods and manually segmented ICV: (a) HD-BET – Manual, (b) SWS – Manual, (c) SynthStrip – Manual, (d) BET2 – Manual. The full lines indicate the mean difference, the dotted lines indicate upper and lower limits of agreement (± 1.96 standard deviations), and the thinner dotted lines in grey represents the zero (no difference).

- [4] Beare RJ, Chen J, Kelly CE, Alexopoulos D, Smyser CD, Rogers CE, et al. Neonatal Brain Tissue Classification with Morphological Adaptation and Unified Segmentation. *Front Neuroinform.* 2016;10:12.
- [5] Hoopes A, Mora JS, Dalca AV, Fischl B, Hoffmann M. SynthStrip: skull-stripping for any brain image. *NeuroImage.* 2022;260:119474.
- [6] Smith SM. Fast robust automated brain extraction. *Hum Brain Mapp.* 2002;17(3):143–55.

A comparative study between in-NICU 1T MRI and conventional 3T MRI

Danielle Sharon¹, [Elizabeth Singh](#)¹, Camilo Jaimes², Patricia Ellen Grant³, Terrie Inder⁴, Mohamed El-Dib^{1,5}

¹Brigham and Women's Hospital, ²Massachusetts General Hospital, ³Boston Children's Hospital, ⁴Children's Hospital of Orange County, ⁵Harvard Medical School

BACKGROUND: In the neonatal period, brain magnetic resonance imaging (MRI) is a valuable clinical tool that offers the ability to visualize brain injury and assess brain growth and development. At the Brigham and Women's Hospital Neonatal Intensive Care Unit (NICU), we began using the Embrace scanner, a 1-Tesla (1T), in-unit MRI clinically in March of 2020. This scanner allows for easier and safer access to brain MRIs for high-risk infants. This retrospective study aims to assess the added diagnostic utility and clinical value of a 3T MRI after obtaining a 1T MRI.

METHODOLOGY: We identified a cohort of infants with an initial MRI in the 1T scanner that had repeat imaging within 14 days in a 3-Tesla (3T) scanner. All infants were admitted to the level III NICU at Brigham and Women's Hospital. The MRIs were done for clinical purposes (per BWH clinical practice guidelines) or as part of research protocols. Follow-up 3T MRIs were performed to obtain higher resolution imaging, magnetic resonance angiogram (MRA), magnetic resonance venography (MRV), or as part of a research protocol. Both clinical and

Figure 1: Comparison between 1T and 3T images in 3 distinct cases. Figures a1-2 (coronal T1) and b1-2 (axial T2) show foci of white matter injury. Figures c1-2 (coronal T2) and d1-2 (axial T2) show hemosiderin staining from prior IVH in the right ventricle. Figures e1-2 (axial DWI) show extensive bilateral fronto-parieto-occipital cerebral diffusion restriction and f1-2 (axial T2) show high signal intensity and loss of white-grey matter differentiation in a case with HIE. WMI; White matter injury, IVH: intraventricular hemorrhage, HIE: Hypoxic ischemic encephalopathy.

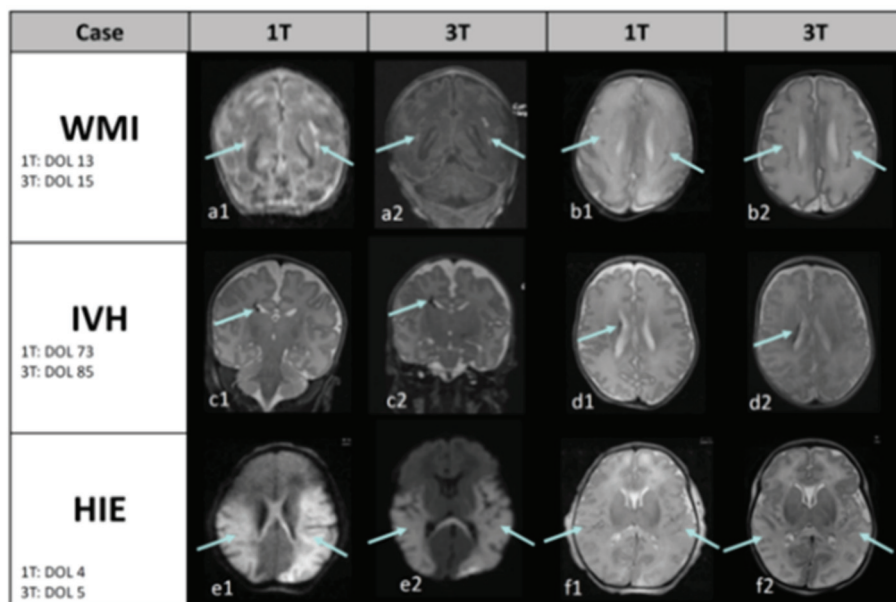


Table 1: Three cases where the 3T MRI differed from the 1T MRI.

Case #	1 Tesla			3 Tesla			Days Between MRIs	Clinical Course
	CGA	Indication	Results	CGA	Indication	Results		
1	43w5d	Apnea	T2 prolongation involving the dorsal aspect of the pons and medulla	44w0d	Better visualization	Abnormality was artifact	2	No change
2	38w0d	Post-TH	Atypical sulci in the parietal and perisylvian regions	38w5d	Better visualization	Improved characterization and extent of malformation	5	No change
3	39w2d	Severe neonatal encephalopathy	Severe HI injury with parenchymal and cerebellar hemorrhages	40w2d	Confirming severity and evolution of injury	Severe HI injury with better visualization and evolution of previously seen hemorrhages	6	Care redirected

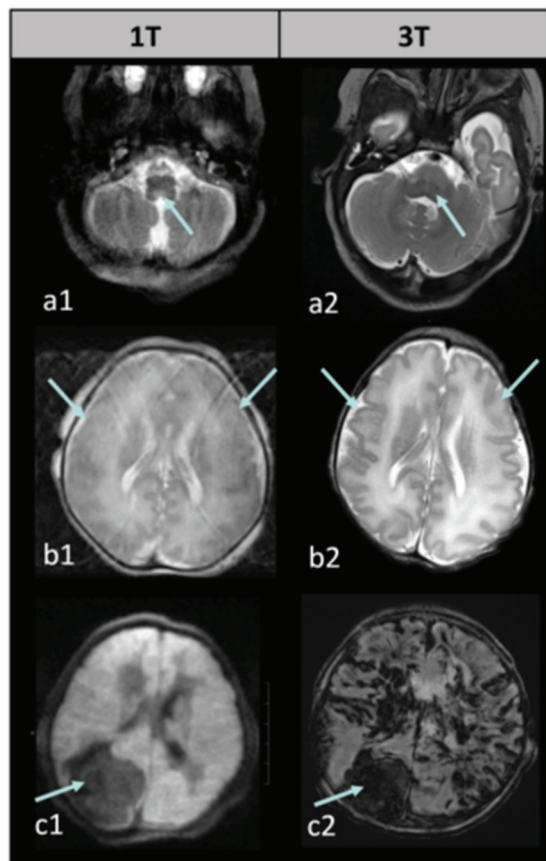
CGA: Corrected Gestational Age, TH: Therapeutic Hypothermia, HI: Hypoxic Ischemic, WMI: White Matter Injury

research MRIs were reported in the same format and were interpreted by pediatric neuroradiologists at Boston Children’s Hospital.

RESULTS: 15 clinical and 19 research MRIs were performed on 1T with 13 scans in full-term infants and 21 in preterm infants (half prior to term equivalent). 26/34 (76%) of the 1T MRIs were interpreted as abnormal. 28

clinical and 6 research MRIs were performed on 3T with 13 scans in full-term infants, 4 in preterm infants prior to TEA, and 17 in preterm infants at TEA. 27/34 (79%) of the 3T scans were found to have an abnormality. In 31 cases (91%), the 3T MRI showed similar or expected evolution of known findings found at 1T (examples in Figure 1). Variation existed in three cases where either an abnormality was defined as artifact, or a more extensive recognition of

Figure 2: Comparison between 1T and 3T images in 3 distinct cases that showed differences. Figure a1 (axial T2) shows T2 prolongation involving the pons and medulla on 1T scan related to motion artifact while a2 (axial T2) shows a normal 3T scan. Figure b1 (axial T2) shows atypical sulci on 1T scan while b2 (axial T2) shows better characterization of immature gyral pattern with areas of abnormal folding at 3T. Figure c1 (diffusion-weighted imaging) shows diffuse restricted diffusion seen throughout the cerebral hemispheres as well as a large right parietal-occipital hemorrhage on 1T while c2 (susceptibility-weighted imaging) shows more extensive parenchymal hemorrhages and persistence of the parieto-occipital hemorrhage on 3T.



injury occurred (Table 1, Figure 2). There appeared to be no clinical impact of the change between the 1T and 3T imaging results.

CONCLUSION: Images from 1T MRI are sufficient for characterizing a wide range of neonatal brain injuries and abnormalities. During the study period, there were limitations associated with the 1T scanner, such as the absence of susceptibility-weighted imaging (SWI) and MRA/MRV. Moreover, in cases involving known or suspected malformations, 3T MRI offers increased signal-to-noise ratio (SNR) allowing increased spatial resolution. However, within our cohort, these limitations did not impact clinical management.

BIBLIOGRAPHY:

Thiim et al., J Perinatol Off J Calif Perinat Assoc. 2022.
Berson et al., Front Neurosci. 2023.
Inder et al., J Pediatr. 2021.

The role of cerebral ultrasound in the identification of potential SARS-CoV-2-associated neonatal brain lesions

Sofia Pellizzari¹, Arianna Zuccato¹, Maria Chiara Bagnato¹, Laura Pecoraro¹, Carlo Alberto Forcellini¹, Mariela Adriana Ventola¹, Elena Bonafiglia¹, Francesca Bissolo¹, Rossella Frassoldati¹, Renzo Beghini¹

¹Neonatal Intensive Care Unit, University Hospital of Verona

BACKGROUND: Background and Purpose: Since the onset of the SARS-CoV-2 pandemic, concerns have arisen regarding the effects of COVID-19 infection during pregnancy. Previous studies have suggested an increased risk of severe complications for both mothers and neonates. However, the specific impact of SARS-CoV-2 on fetal brain development remains unclear. This study aims to investigate the influence of SARS-CoV-2 infection during pregnancy on neonatal neurological outcomes, with a focus on neuroradiological features detectable through a non-invasive method, such as cerebral ultrasound. The research also seeks to assess the risk of specific brain lesions in neonates exposed to the virus, considering various factors, including gestational age at the time of infection, the severity of maternal COVID-19 symptoms, maternal vaccination status, and the presence of placental histological lesions.

METHODOLOGY: Conducted at the Ospedale della Donna e del Bambino in Verona, this prospective observational cohort study included neonates born between January 2022 and May 2023, born at or after 34 weeks of gestation and without diagnoses of TORCH infections or congenital malformations. All newborns underwent cerebral ultrasound within ten days of birth. A follow-up examination was conducted at one month for SARS-CoV-2-exposed neonates. Ultrasound images of standard sagittal and coronal planes were obtained. Statistical analysis was performed using STATA software.

RESULTS: The study enrolled a total of 240 subjects, including 118 neonates exposed to SARS-CoV-2 during pregnancy and 122 unexposed neonates. Among the observed brain lesions, lenticulostriate vasculopathy was the most common in exposed neonates (8,5%). The frequent occurrence of this vasculitic and progressive brain lesion supports the hypothesis of a correlation with inflammation-related placental pathology caused by

SARS-CoV-2. Other abnormalities, such as focal echogenicities, intraventricular hemorrhages, and subependymal cysts, were also identified. The study revealed that in utero exposure to SARS-CoV-2 is significantly associated with presence of these ultrasound brain lesions (p-value=0.007, =0.05). The relative risk of brain injury in the exposed population was 3.87, with an Odds Ratio of 4.2. The SARS-CoV-2 exposure was also significantly associated with the presence of placental histopathological lesions (p-value <0.001), and these were significantly associated with the presence of ultrasound lesions (p-value=0.023).

CONCLUSION: This study's findings suggest that neonates exposed to SARS-CoV-2 in utero face an increased risk of developing brain abnormalities detectable through cerebral ultrasound, including lenticulostriate vasculopathy, subependymal cysts, and intraventricular hemorrhages. These results underline the importance of preventing SARS-CoV-2 infection during pregnancy, potentially necessitating closer monitoring of virus-exposed fetuses. Moreover, they emphasize the need for postnatal neurological follow-up for neonates exposed to the virus at birth. These findings open new research perspectives into the effects of COVID-19 and congenital viral infections on fetal, neonatal, and infant health, encouraging further studies for a better understanding of long-term effects.

Neural mechanisms underlying emotion processing and autistic traits during task-based fMRI following very preterm birth

Marguerite Leoni^{1,2}, Lucy Vanes^{1,2}, Anais Durand^{1,2}, Laila Hadava^{1,2}, Chiara Nosarti^{1,2}

¹Centre for the Developing Brain, School of Biomedical Engineering & Imaging Sciences, King's College London, ²Department of Child and Adolescent Psychiatry, Institute of Psychiatry Psychology and Neuroscience, King's College London

BACKGROUND: Very preterm birth (VPT; <32 weeks' gestation) is associated with altered brain development and behavioural problems such as facial emotional processing. In addition, VPT born participants are at significantly greater risk of being diagnosed with autism spectrum disorder (ASD) compared to their full-term (FT) born peers. In this study, whole brain activation and its association with dimensional ASD traits was assessed in VPT and FT children in a implicit facial emotional processing task-based fMRI paradigm.

METHODOLOGY: 83 VPT and 61 age-matched FT participants (7-11 years old) underwent an implicit facial

emotion processing functional magnetic resonance imaging (fMRI) task to explore hemodynamic responses associated with facial emotion processing in association with autistic-like difficulties with social communication and interaction (SCI). These were assessed using the Social Responsiveness Scale – 2nd edition (SRS-2).

RESULTS: VPT participants displayed hyperactivation in the right superior frontal and mid occipital gyri when processing angry and fearful faces (compared to neutral faces), respectively. Whole brain analyses revealed that increased social communication difficulties in both VPT and FT participants were associated and with reduced activation of the left superior and inferior occipital gyri when processing faces (compared to shapes), and with increased activation in the right fusiform gyrus when processing angry (compared to neutral) faces. In contrast, VPT participants showed a positive association between social communication deficit and activation in left mid-temporal gyrus when processing fearful (compared to neutral) faces, while this association was reversed in FT participants.

CONCLUSION: Our results highlight both overlapping and distinct mechanisms underlying social communication deficits in preterm and full-term children. Group differences between FT and VPT emerged particularly in brain areas associated with processing emotions and first-level face processing. On the other hand, differences related to increased social communication difficulties in whole brain analyses were seen in VPT children in brain regions involved in the "social brain" and face-specific areas. VPT brain activation during facial emotional processing seems unique to this population as it differs significantly from FT.

Risk of severe intraventricular hemorrhage in premature infants with prenatal exposure to illicit substance/s.

Divya Rana¹, Mimily Harsono, Massroor Pourcyrus¹

¹University of Tennessee Medical Science Center

BACKGROUND: Maternal substance use disorder (SUD) is a major public health concern, particularly in united States with rising use of illegal synthetic opioids as well as legalization of marijuana. SUD during pregnancy increases risk of stillbirth, birth defects, low birth weight and premature birth. Use of one or more substance/s. which easily cross placenta, have neurovascular pharmacodynamic effects and can potentially increase risk of severe intraventricular hemorrhage (IVH). Published reports on infants with gestational age (GA) <32 weeks or birth weight (BW) <1500 grams showed incidence of all

grades IVH remains at ~25 % and severe-IVH at ~7.7%. However, the incidence of IVH in premature neonates exposed to illicit substance/s is unknown.

OBJECTIVE: We hypothesized that fetal exposure to illicit substance/s will increase risk of IVH in premature infants.

METHODOLOGY: This is a prospective cohort study of Cranial Ultrasound (CUS) findings in preterm infants who had in-utero illicit substance/s exposure. Serial CUS are obtained within first 14 days, at 21-30 days-of-life and at corrected-GA of 36 weeks. We included all live birth with

GA <32wk or BW <1,500g that were born in 2014 - 2020. In-utero illicit drug exposed infants were identified from maternal history, maternal urine toxicology test and confirmed with post-natal umbilical cord tissue toxicology test. We excluded complex congenital and chromosomal anomalies infants.

RESULTS: 1,164 infants (GA <32wk or BW <1,500g) were born in our maternity Hospital from 2014 - 2020. We considered CUS to be abnormal based on the worst grade identified in the first 30 days-of-life. The incidence of IVH in non-exposed infants was as follows: grade I 19.6%, grade II 7.8%, grade III 2.9% and grade IV 6.3%. We

Table 1 Characteristic of Illicit Drug Exposed Premature Infants (n=55)		
Gestational Age (weeks; mean ± SD)		28.4 ± 2.6
Birth Weight (grams; mean ± SD)		1,072.5 ± 330.9
Gestational Age (weeks)	22-23	3.6% (2/55)
	24-25	16.4% (9/55)
	26-27	18.2% (10/55)
	28-29	30.9% (17/55)
	30-31	23.6% (13/55)
	32-33	7.3% (4/55)
Gender	Male	49.1% (27/55)
Race	Black	85.5% (47/55)
Delivery Mode	Cesarean-section	63.6% (35/55)
	Spontaneous vaginal	36.4% (20/55)
	In-born or hospital birth	96.4% (53/55)
Antenatal Betamethasone		74.5% (41/55)
Antenatal Magnesium sulfate		69.1% (38/55)
Apgar Score	at 1 min	5 (IQR 2-7)
	at 5 mins	8 (IQR 6-9)
	at 1 min < 4	30.9% (17/55)
	at 5 min < 4	3.6 (2/55)
Cranial Ultrasound (days)	1 st CUS	7.5 ± 4.6
	2 nd CUS	22.8 ± 4.7
	3 rd CUS	53.4 ± 7.3
Cranial Ultrasound Findings	Low grade IV (grade-I & II)	52.7% (29/55)
	Severe IVH (grade-III & IV)	1.8% (1/55)
	Cerebellum Hemorrhage	3.6% (2/55)
	Lenticulostriate vasculopathy	1.8% (1/55)
	Arachnoid cyst	1.8% (1/55)
Exposed Illicit Substance/s	Polydrug	38.2% (21/55)
	Opioids	49.1% (27/55)
	Cannabinoids	43.6% (24/55)
	Cocaine	30.9% (17/55)
	Methamphetamine	5.5% (3/55)
	Barbiturate	10.9% (6/55)
	Benzodiazepine	3.6% (2/55)
Maternal age & medical condition	Age (Years; mean ± SD)	27.9 ± 6.5
	Pre-eclampsia	30.9% (17/55)
	Hypertension	18.2% (10/55)
	Abruptio Placenta	9.1% (5/55)
	Preterm Labor	32.7% (18/55)
	Preterm Prolonged Rupture of Membranes (PPROM)	20% (11/55)

Data are presented as mean ± SD; n/total (%); or median and IQR.

identified 55 infants that were exposed prenatally to illicit substance/s. Of the exposed infants, 58.2% (32/55) had abnormal CUS; compared to non-exposed; the incidence of IVH was as follows: grade I 43.6% [p<0.01; OR 3.89, 95% CI 2.11-7.17], grade II 9.1% [p=0.09; OR 2.02, 95% CI 0.74-5.52], grade III 1.8% [p=0.46; OR 1.1, 95% CI 0.14-8.44] and no grade IV IVH [p=0.33; OR 0.24, 95% CI 0.01-4.07]. Maternal-Infant characteristics (Table 1).

CONCLUSION: Low grade IVH (grade 1 and 2) was noted in majority of the illicit substance/s-exposed premature infants, and severe IVH (grade 3 and 4) was lower compared to non-exposed infants. We plan to further investigate the severity of IVH and its correlation with the drug of abused, umbilical cord drug concentrations, maternal lifestyle, and other relevant medical-social issues.

Early and term-equivalent age MRI in detection of white matter injury in very preterm infants

Sriya Roychaudhuri^{1,2}, Gabriel Cote-Corriveau^{1,3}, Carmina Erdei^{1,4}, Terrie Inder^{1,4,5}

¹Division of Newborn Medicine, Department of Pediatrics, Brigham and Women’s Hospital,

²Division of Neonatal-Perinatal Medicine, Department of Pediatrics, Surrey Memorial Hospital, University of British Columbia,

³Department of Pediatrics, Sainte-Justine University Hospital Center, ⁴Harvard Medical School,

⁵Division of Neonatology, Children’s Hospital of Orange County and Department of Pediatrics, University of California

BACKGROUND: White matter injury (WMI) in infants born preterm is the most prevalent form of injury and associated with adverse neurodevelopmental outcomes.

Magnetic resonance imaging (MRI) has distinct advantages over routine cranial ultrasound to visualize WMI in the initial weeks following preterm birth and at term-equivalent age (TEA). Systematic MRI scoring methods to assess the extent of WMI have been proposed for both early and TEA times. Early MRI interpretation focuses on characterization of the number and size of the WMI lesions (1), whereas TEA MRI captures sequelae of prior injury such as cystic lesions, signal abnormalities, delayed myelination and white matter volume loss (2).

OBJECTIVE: To compare WMI on early brain MRI, at 30 to 34 weeks post-menstrual age (PMA), with WMI assessment at TEA (37-42 weeks PMA) MRI, using two standardized scoring systems, in infants born < 33 weeks gestational age (GA).

MATERIALS AND METHODS: The Miller et al (1) scoring was used for categorization of injury on early MRI. TEA MRIs were assessed for WMI and its sequelae using the Kidokoro et al (2) score. The degree of WMI and global injury were categorized as normal-mild and moderate-severe. Global injury scores consider presence and degree of intraventricular hemorrhage and ventricular dilation along with WMI. We assessed the relationship between early and TEA classifications using Fisher’s exact tests.

RESULTS: The cohort consisted of 30 infants with mean GA of 28.7 weeks and median birthweight of 1220 grams. The early MRIs were performed at an average of 33.0 weeks (SD = 1.4), and the TEA MRIs at 38.6 weeks (SD = 1.4) PMA (Figure 1). There was a strong association between the systematic assessments of global injury severity (p < 0.001) and WMI (p=0.007) at the two time points (Table 1)(Figure 2). There was no instance of newly detected WMI or increased lesion severity noted on TEA when compared to early MRI scans.

CONCLUSION: Evaluating brain injury using standardized scoring systems enables clinicians and

Table 1 Comparison of WMI and global assessments on early vs. TEA MRI^a

(A)		WMI severity on TEA MRI		(B)		Global severity on TEA MRI	
		Normal-Mild (n = 20)	Moderate-Severe (n = 10)			Normal-Mild (n = 19)	Moderate-Severe (n = 11)
WMI severity on early MRI	Normal-Minimal (n = 22)	18	4	Global severity on early MRI	Normal-Mild (n = 19)	18	1
	Moderate-Severe (n = 8)	2	6		Moderate-Severe (n = 11)	1	10

TEA: Term-equivalent age; WMI: White matter injury.

^aComparison of (A) WMI severity categories and (B) global severity categories on early and TEA MRI.

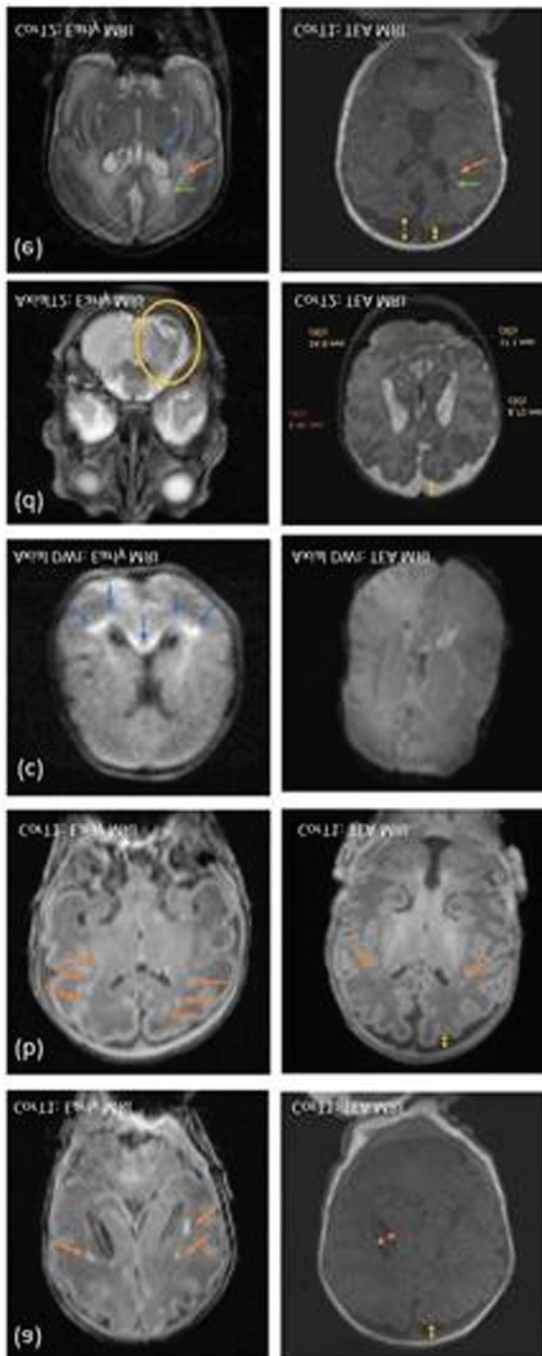


Figure 1: The figure illustrates WMI as appreciated in early (1 Tesla scanner) vs. TEA MRI (3 Tesla scanner) in different cases. (a) The image on the left shows an early MRI and the extent of WMI (orange arrows) and its evolution at TEA (image on the right) where there is an absence of visible WM lesions. WMI sequelae can be appreciated as volume loss, with arrows indicating dilated ventricle and enlarged sub-arachnoid space (yellow arrow). (b) Early T1 images showing severe WMI (orange arrows) with reduced conspicuity at TEA but with some volume loss. (c) Early MRI at day three of life showing diffusion restriction in WM (blue arrows) which has resolved at TEA. (d) Isolated unilateral significant cerebellar hemorrhage (encircled in yellow) with eventual disparity in cerebellar hemispheric sizes and bilateral cerebral WM volume loss at TEA. (e) Early IVH (blue arrow) with dilatation resulting in periventricular WMI (orange arrows) with cyst formation (green arrows) and volume loss at TEA.

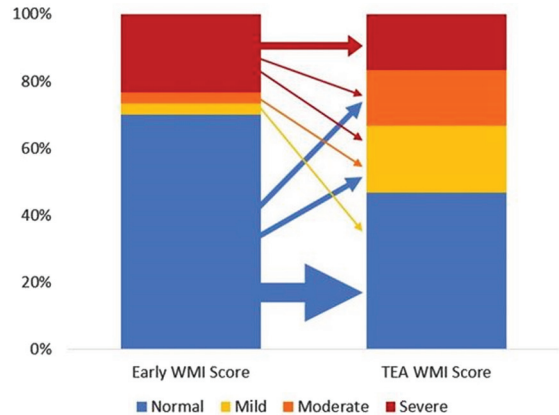


Figure 2: Evolution of WMI severity categories from early to TEA MRI^a

TEA: Term-equivalent age; WMI: White matter injury.

^aThe thickness of arrows is proportional to the number of cases.

researchers to analyze images in a systematic manner and follow WMI longitudinally in very preterm infants. Although the optimal timing to undertake neuroimaging in the preterm infant remains to be determined, early (30-34 weeks) and TEA MRI may independently provide valuable information on WMI and risk for associated sequelae.

BIBLIOGRAPHY:

1. Miller SP, Ferriero DM, Leonard C, Piecuch R, Glidden DV, Partridge JC, et al. Early brain injury in premature newborns detected with magnetic resonance imaging is associated with adverse early neurodevelopmental outcome. *J Pediatr.* 2005 Nov;147(5):609–16.
2. Kidokoro H, Neil JJ, Inder TE. New MR imaging assessment tool to define brain abnormalities in very preterm infants at term. *AJNR Am J Neuroradiol.* 2013;34(11):2208–14.

Intraventricular brain hemorrhage detection through transfontanelle photoacoustic imaging: An innovative approach

Juliana Benavides¹, Rayyan Manwar¹, Laura S. McGuire², Tarikul Islam¹, Anthony Shoo³, Fady T. Charbel², Martha G. Menchaca³, Amanda P. Siegel¹, De-Ann M. Pillers³, Juri G. Gelovani⁴, Karman Avnaki¹

¹Richard and Loan Hill Department of Bioengineering, Richard and Loan Hill Department of Bioengineering, University of Illinois at Chicago, ²Department of Neurological Surgery, University of Illinois at Chicago – College of Medicine, ³Section of Neonatology, Department of Pediatrics, UIHealth Children’s Hospital of the University of Illinois at Chicago, ⁴Provost Office, College of

Medicine and Health Sciences, United Arab Emirates University

SUMMARY: The capability of transfontanelle photoacoustic imaging (TFPAI) to detect intraventricular and periventricular hemorrhages has been demonstrated in a sheep brain model in-vivo.

BACKGROUND AND OBJECTIVE: In preterm neonates, intraventricular (IVH) and periventricular (PVH) hemorrhages are common due to the fragility of undeveloped periventricular blood vessels. While transfontanelle ultrasound has been utilized for initial screenings of the brain through the anterior fontanelle, its reliability in diagnosing mild hemorrhages remains uncertain. Inconclusive diagnoses are common in those cases, leading to potential oversight and increased risks of moderate to severe neurodevelopmental complications. This study demonstrates the capability of photoacoustic (PA) imaging to detect IVH/PVH volumes as small as 0.3 mL of blood in the brain.

METHODOLOGY: A cranial window, simulating the neonatal fontanelle, was created in an adult sheep model with a diameter of 2.5 mm. The hemorrhage was induced by injecting heparinized arterial blood into the left lateral ventricle in volumes ranging from 0.1 to 1.0 mL in increments of 0.1 mL. Photoacoustic images were acquired at a 798 nm wavelength (isosbestic point for oxyhemoglobin and deoxyhemoglobin) after each injection.

RESULTS: In both IVH and PVH models, photoacoustic average intensity showed a linear increase corresponding to the increment of the injected volumes of blood, effectively detecting mild hemorrhages. For IVH model, it was detected volumes as small as 0.3 mL and 0.2 mL for the two animals used in the study. In contrast, the PVH mode showed detection at 0.2 mL and 0.3 mL respectively. Comparative analysis with ultrasound data revealed that IVH signals were detectable in cerebrospinal fluid (CSF) at 0.5 mL, which corresponds to 5% bleeding, aligning with clinical neonatal studies. For the PVH model, ultrasound detection started at an injection of 0.4 mL. While both methods identified IVH and PVH in vivo, TFPAI demonstrated superior sensitivity in detecting smaller hemorrhages.

CONCLUSION: The results demonstrate that the TFPAI signal intensity is strongly correlated with the concentration of blood in ventricular CSF and volume of blood in a periventricular lesion. In addition, the comparison with the results from the ultrasound imaging showed that the photoacoustic imaging modality has higher sensitivity for the detection of mild hemorrhages in both models IVH and PVH. Future steps aim to refine blood measurement accuracy in CSF through alternative image reconstruction algorithms, compensating for non-linear effects to enhance

the precision of weak PA signals. We expect that the TFPAI probe will be a valuable monitoring tool especially for neonates with critical conditions and admitted into intensive care unit (NICU).

Hemodynamic responses associated with spontaneous neural activity in the early developing brain

Anna Shiraki^{1,2}, Hama Watanabe³, Gentaro Taga³, Misa Hashimoto¹, Misae Yamada¹, Hajime Narita¹, Takamasa Mitsumatsu¹, Sumire Kumai¹, Ryosuke Suzui¹, Fumi Sawamura¹, Takashi Maeda⁴, Yuji Ito¹, Hiroyuki Yamamoto¹, Tomohiko Nakata¹, Yoshiaki Sato⁴, Jun Natsume^{1,5}, Hiroyuki Kidokoro¹

¹Department of Pediatrics, Nagoya University Graduate School of Medicine, ²Department of Pediatrics, Nagoya Memorial Hospital, ³Graduate School of Education, The University of Tokyo, ⁴Division of Neonatology, Center for Maternal-Neonatal Care, Nagoya University Hospital, ⁵Department of Developmental Disability Medicine, Nagoya University Graduate School of Medicine

BACKGROUND AND OBJECTIVE: Delta brushes are prominent intrinsic activities observed in the electroencephalogram (EEG) of preterm infants, typically between 32 and 36 weeks of postmenstrual age (PMA). These spontaneous neural activities are believed to be associated with the activity of subplate neurons, which is crucial for early brain development. However, it remains unclear whether the specific brain regions respond to these localized neural activities. We aimed to explore hemodynamic responses associated with delta brushes in preterm EEG using simultaneous EEG and functional near-infrared spectroscopy (fNIRS) recordings.

METHODOLOGY: We enrolled 17 infants whose gestational ages ranged from 30 to 34 weeks. EEG-fNIRS recordings were conducted at two time points: 34 and 36 weeks of PMA, with a median analysis duration of 50 min.

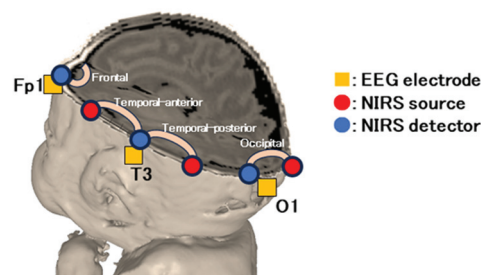


Figure 1. Electroencephalography (EEG) and near-infrared spectroscopy (NIRS) setup. NIRS channels were positioned directly above the line connecting Fp1, T3, O1, O2, T4 and Fp2 EEG electrodes.

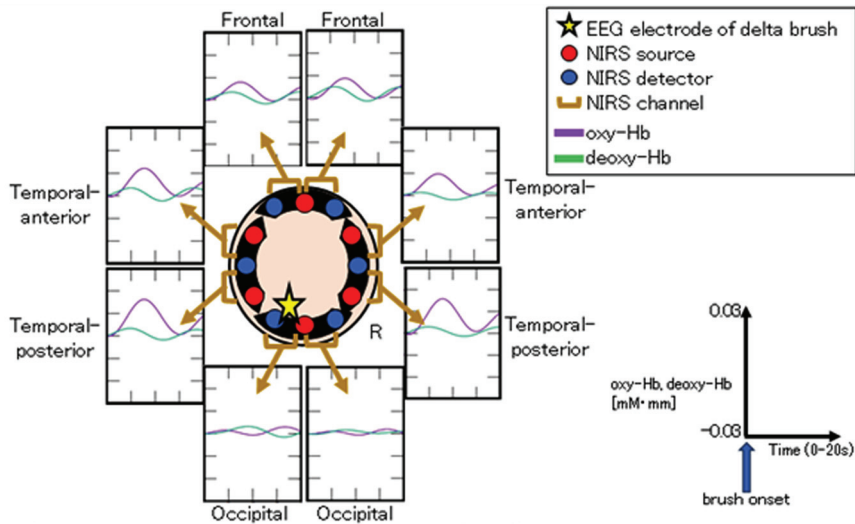


Figure 2. Group analysis data of grand averages for left occipital brushes. A part of the group analysis conducted during quiet sleep at 36 weeks of postmenstrual age. NIRS channels were categorized based on their positions. Similar analyses were conducted for other EEG electrodes during both active and quiet sleep.

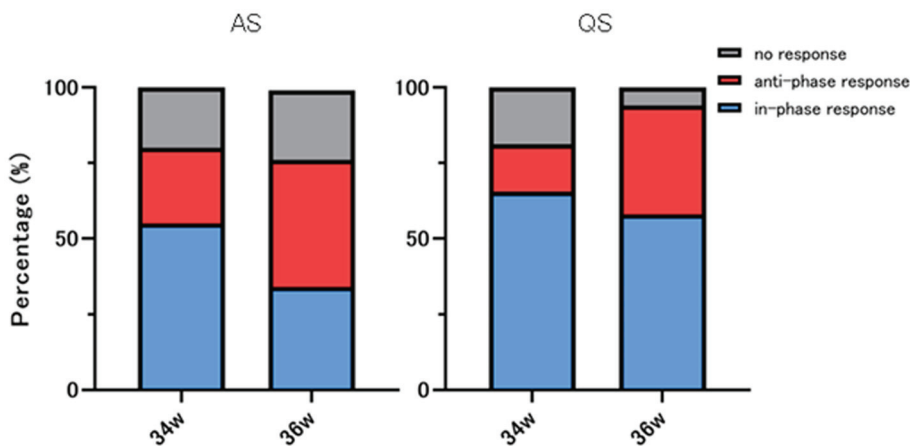


Figure 3. Comparison of hemodynamic responses between the 34-week and 36-week postmenstrual age groups. In both active sleep (AS) and quiet sleep (QS), the anti-phase response was significantly more prominent in the 36-week group than in the 34-week group ($p = 0.017$ and 0.027 , respectively).

EEG was recorded polygraphically with eight electrodes (Fp1, Fp2, C3, C4, O1, O2, T3 and T4) to distinguish active sleep (AS) from quiet sleep (QS). To identify the brush component of delta brushes in the bipolar EEG envelope, we developed an automated detection algorithm. This algorithm filtered EEG at 8–25 Hz and detected brushes with durations of 0.3–1.5 s and average amplitudes exceeding 10 μV within a sliding window of 0.3 s. An eight-channel NIRS device was placed around the head to measure changes in oxy- and deoxy-hemoglobin concentrations (Fig. 1). Hemodynamic grand averages were calculated for localized brushes in each NIRS channel during both AS and QS in each recording.

Subsequently, we conducted group analyses based on the PMA at the time of recording (Fig. 2). The group analysis data were classified into three responses according to the relationships between oxy- and deoxy- hemoglobin changes: in-phase, anti-phase, and no response. We also investigated the associations between these hemodynamic responses, the PMA at the time of recording, and NIRS channel positions, including frontal, temporal-anterior, temporal-posterior, and occipital areas.

RESULTS: Among the 64 grand average data sets for each PMA group and sleep state, over 75 % displayed hemodynamic changes associated with localized delta

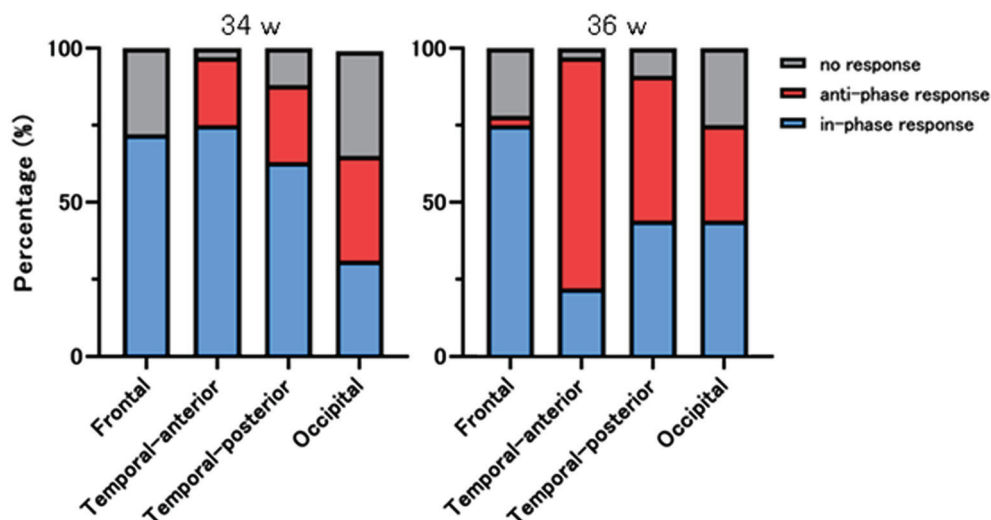


Figure 4. Comparison of hemodynamic responses across NIRS positions. At 34 and 36 weeks, the anti-phase response was significantly less pronounced in the frontal regions compared to other regions. In contrast, at 36 weeks, the anti-phase response was significantly more prominent in the temporal-anterior regions ($p < 0.001$).

brushes (Fig. 3). At 36 weeks of PMA, there was a higher prevalence of anti-phase responses observed in both AS and QS. Considering NIRS channel positions, the temporal-anterior regions exhibited a more pronounced hemodynamic response rate in both the 34 and 36-week PMA groups (Fig. 4). Notably, the increased prevalence of anti-phase responses in the temporal-anterior regions at 36 weeks of PMA.

CONCLUSION/IMPACT: Delta brushes were associated with hemodynamic responses in broad areas as early as 34 weeks of PMA. These responses shifted from an in-phase to an anti-phase pattern as the brain matured. The increased rate and prevalence of anti-phase responses in the temporal-anterior regions indicate the involvement of the insula, a most strongly interconnected hub in the developing brain.

Contemporary patterns of brain injury in infants with neonatal encephalopathy in the therapeutic hypothermia era

Aisling Garvey^{1,2}, Eniko Szakmar^{2,3}, Hoda El-Shibiny², H el ene Meunier⁴, Brian Walsh^{1,2,5}, Sara Cherkerzian², Mohamed El-Dib², Terrie Inder^{2,6}

¹Infant Research Centre, ²Department of Pediatrics, Division of Newborn Medicine, Brigham and Womens Hospital, Harvard Medical School, ³1st Department of Pediatrics, Semmelweis University, ⁴Department of Neonatology, Alix de Champagne, ⁵Department of Neonatology, Cork University

Maternity Hospital, ⁶Childrens Hospital of Orange County, University of California Irvine

BACKGROUND: Brain injury in Neonatal Encephalopathy (NE) has historically been classified into injury to the deep grey matter, white matter/watershed area or global injury (1). However, injury in other areas have been described (2,3). This study aimed to describe contemporary patterns of brain injury in infants with NE in the era of therapeutic hypothermia (TH) and to examine potential risk factors associated with different patterns of injury.

METHODOLOGY: Retrospective analysis of all infants with NE admitted for TH to the Brigham and Women’s Hospital, a tertiary NICU (January 2016-December 2021). MRIs were performed after rewarming and scored independently by 3 reviewers blinded to outcome and grade of encephalopathy using the Weeke scoring system (2). Mann-Whitney U Tests were performed to compare risk factors in infants with and without different patterns of injury.

RESULTS: Two-hundred and eighty-nine infants with all grades of NE were included with a median gestational age of 39.3weeks (IQR 37.5-40.1) and median birthweight of 3.13kg (IQR 2.72-3.54). Of these, 196 (68%) had abnormal MRI findings. Locations of injury are outlined in Table 1. Injury to the grey matter was associated with the requirement for extensive resuscitation (chest compressions $p < 0.001$, epinephrine $p < 0.001$), lower 10-minute Apgar scores ($p = 0.003$), worse post-natal gas measurements (pH $p = 0.043$, base deficit $p = 0.033$, lactate $p = 0.031$) and the requirement for inotropes in the NICU ($p = 0.013$).

n (%)	
MRI Findings	
Normal MRI (score of 0)	93 (32)
Abnormal MRI (score of ≥ 1)	196 (68)
Location of Injury	
n (% of those with injury)	
Deep Grey Matter	
Thalamus	22 (11)
Basal Ganglia	23 (12)
PLIC	22 (11)
Brainstem	6 (3)
Perirolandic Cortex	11 (6)
Hippocampus	7 (4)
White Matter	
Cortex	32 (16)
White Matter (not PWML)	47 (24)
PWML	32 (16)
Hemorrhage	26 (13)
Optic Radiation	16 (8)
Corpus Callosum	22 (11)
Cerebellar	
Signal abnormalities	12 (6)
Hemorrhage	32 (16)

PLIC, posterior limb of the internal capsule; PWML, punctate white matter lesions

Injury to the white matter was associated with a lower birthweight ($p=0.005$), risk of chorioamnionitis ($p=0.033$), lower umbilical pH values ($p<0.001$), lower 5- and 10-minute Apgar scores ($p=0.021$ and 0.015 respectively) and the requirement for intubation ($p=0.004$). Infants with grey or white matter injury had a higher clinical ($p=0.003$, $p=0.001$) and EEG grade ($p=0.002$, $p=0.048$) of NE and were more likely to require intubation ($p=0.022$, $p=0.004$). These infants had a higher incidence of seizures ($p<0.001$) and death ($p=0.003$), and had longer hospital stays ($p<0.001$). Cerebellar injury was associated with vaginal delivery ($p=0.043$) and incidence of PPV ($p=0.043$).

CONCLUSION: Areas of brain injury noted in infants with NE extend beyond the hallmark patterns of basal ganglia/thalamus and watershed areas and are associated with different risk factors which may aid in the short-term prediction of outcome.

BIBLIOGRAPHY:

1. Barkovich AJ, Hajnal BL, Vigneron D, Sola A, Partridge JC, Allen F, et al. Prediction of neuromotor outcome in perinatal asphyxia: evaluation of MR scoring systems. *AJNR*. 1998;19(1):143-9
2. Weeke LC, Groenendaal F, Mudigonda K, Blennow M, Lequin MH, Meiners LC, et al. A Novel Magnetic Resonance Imaging Score Predicts Neurodevelopmental Outcome After Perinatal Asphyxia and Therapeutic Hypothermia. *J Pediatr*. 2018;192:33-40.e2
3. Wisnowski JL, Wintermark P, Bonifacio SL, Smyser CD, Barkovich AJ, Edwards AD, et al. Neuroimaging in the term newborn with neonatal encephalopathy. *Semin Fetal Neonatal Med*. 2021;26(5):101304

Magnetic resonance imaging and proton spectroscopy predicts neurodevelopmental impairment outcomes after neonatal encephalopathy in Uganda

Samantha Sadoo¹, Carol Nanyunja¹, Ivan Mambule², Emily Webb¹, Jamiir Mugalu³, Alan Bainbridge⁴, Kelly Pegoretti Baruteau⁵, Francisco Torrealdea⁴, Latha Srinivasan⁵, Allena Nabawanuka⁶, Gilbert Gilbert⁷, Sean Mathieson⁸, Joe Bwambale⁶, Samson K Lubowa⁶, Huzair Ssesembo⁶, Pia Wintermark¹⁰, Geraldine Boylan⁸, Moffat Nyirenda², Nicola Robertson¹¹, Michael Kawooya¹³, Frances Cowan¹², Annetee Nakimuli⁹, **Cally Tann¹**

¹London School of Hygiene & Tropical Medicine, ²MRC/UVRI & LSHTM Uganda Research Unit, ³Kawempe National Referral Hospital, ⁴University College London, ⁵University College London Hospital, ⁶Kampala MRI Centre, ⁷MRC Clinical Science, Philips Healthcare, ⁸INFANT Research Centre, University College Cork, ⁹Makerere University, ¹⁰McGill University, ¹¹University of Edinburgh, ¹²Imperial College London, ¹³Ernest Cook Ultrasound Research and Education Institute (ECUREI)

BACKGROUND: Intrapartum-related neonatal encephalopathy (NE) is a leading cause of child death and disability globally, especially in low-income countries where therapeutic hypothermia is frequently unavailable (1). Neonatal brain magnetic resonance imaging and spectroscopy (MRI/MRS) are key tools for brain injury detection, assessment, and prognostication (2). We assessed feasibility and acceptability of MRI/MRS and predictive validity for adverse neurodevelopmental outcome after NE in Uganda.

METHODOLOGY: Neonates were recruited to a prospective cohort study ("Baby BRAiNS") at a tertiary referral facility in Kampala, Uganda(3). Participants had NE (Thompson score ≥ 5 ; ≥ 36 weeks; ≥ 1.8 kg; resuscitation at birth) and underwent MRI/MRS at around day 10 of life (1.5 Tesla) after collaborative protocol development and training (3). Images were evaluated for diagnostic quality, injury pattern and severity, and scored using Rutherford and NICHD criteria (4, 5). Basal ganglia and thalamus (BGT) MRS were analysed for peak area metabolite ratios, including lactate, N-acetylaspartate (NAA), creatine, and choline, using Tarquin. Adverse outcome (18-24 months) was defined as death or moderate-severe neurodevelopmental impairment; Bayley-III cognitive/motor score < 70 , Hammersmith Infant Neurological Examination < 67 , and/or GMFCS level 3-5. Optimal MRI

Table 1: Baseline characteristics of participants

Characteristic	MR imaged (n=27)	Not imaged (n=24)	All (n=51)	p-value
Gestational age, median (IQR)	40 (38-40)	38 (38-40)	38 (38-40)	0.98
Birthweight (g), median (IQR)	3030 (2710-3500)	3000 (2830-3240)	3010 (2800-3400)	0.73
5-minute Apgar score <6, % (n)	22.2% (6)	62.5% (15)	41.2% (21)	0.01
Modified-Sarnat staging, % (n)				
1 - Mild	33.3% (9)	9% (2)	21.6% (11)	0.02
2 - Moderate	37.0% (10)	20.8% (5)	29.4% (15)	
3 - Severe	25.9% (7)	62.5% (15)	43.1% (22)	
EEG background score, % (n)				
0 - Normal limits	3.7% (1)	4.4% (1)	3.9% (2)	0.008
1 - Mild	44.4% (12)	17.4% (4)	31.4% (16)	
2 - Moderate	18.5% (5)	16.7% (4)	17.6% (9)	
3-4 - Severe	33.3% (9)	61.0% (14)	45% (23)	
Electrographic seizures, % (n)	48.1% (13)	54.2% (13)	51% (26)	0.58
Neonatal death, % (n)	0.0% (0)	59.1% (13)	26.5% (13)	<0.0001

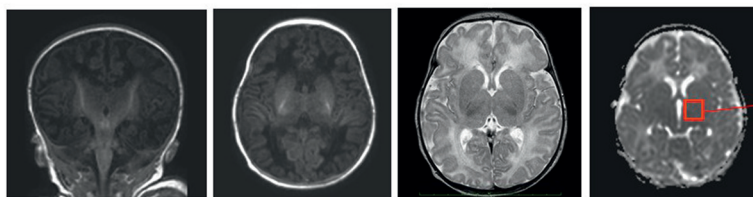
score/MRS ratio thresholds for prediction of outcomes were identified through ROC curve analysis, and predictive validity assessed.

RESULTS: Of 51 participants, 27 consented for and underwent MRI, and 24 MRS (median 11 days, IQR 11-16.4), all of diagnostic quality: providing evidence of feasibility and acceptability. Twenty-four were not imaged due to death before scan (13), Covid-19 lockdown (6), failure to attend (3), and withdrawal (2). Of those imaged, 21 had outcome data (1 death; 5 adverse; 15 favourable).

Non-imaged infants had more severe NE, EEG background, and higher mortality (Table 1). Abnormalities were seen in 93% (26); 84% (22) showed hypoxia-ischaemia, none showed antenatal injury. Severe abnormalities were seen equally in the BGT and white matter (14.8%). Of the 7 (26%) predictive of adverse outcome (Rutherford), 6 had adverse outcome on follow-up (Figure 1). Rutherford score ≥ 7 and NICHD $\geq 2A$ were both predictive of adverse outcome (Figure 2). MRS metabolite ratios were significantly different in the adverse compared to favourable outcome groups ($p=0.01, 0.006, 0.009$). Sensitivity and

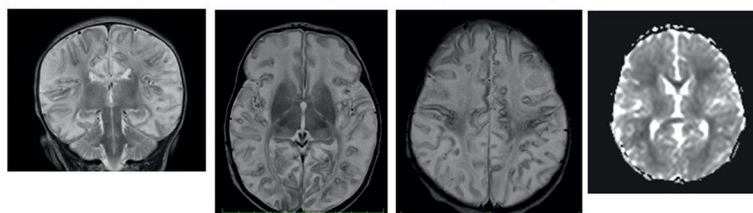
Figure 1: MRI and MRS images from two participants with (A) Favourable outcome, and (B) Adverse outcome

(A) 42 weeks' gestation; scanned day 11. MRI T2 (coronal, axial), ADC, MRS



MRI: Diffuse white matter changes bilaterally, with increased diffusibility on ADC map, total injury score 2. MRS: Lac:NAA 0.08

(B) 38 weeks' gestation; scanned day 11. MRI T2 (coronal, axial), ADC, MRS



MRI: Severe widespread cortical and white matter injury, mild basal ganglia and thalami changes, low signal in white matter and thalami on ADC, total injury score 8. MRS: Lac:NAA 0.26

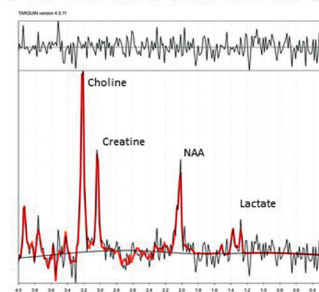
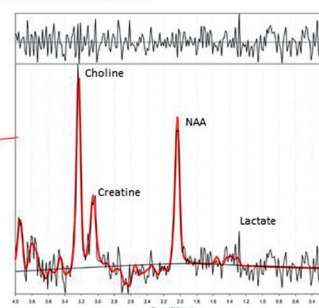
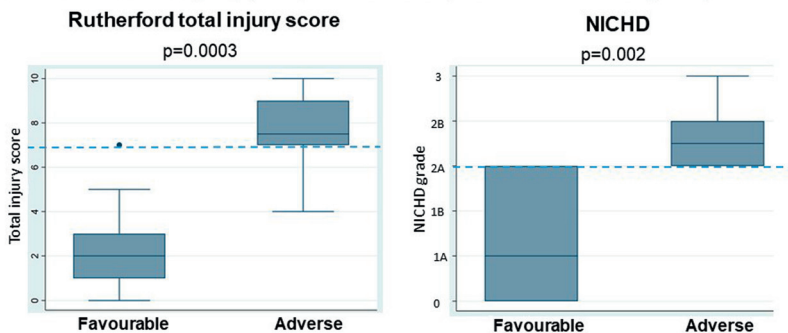


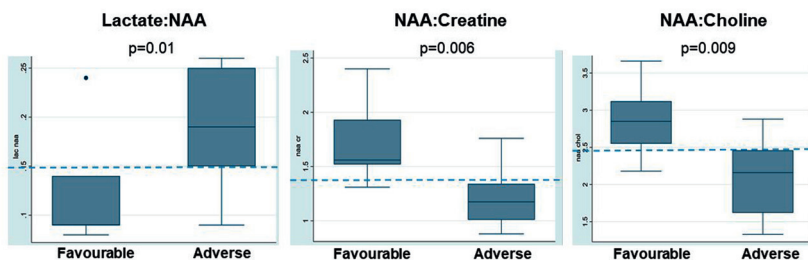
Figure 2: MRI Rutherford/NICHD injury scores: comparing distributions of scores between favourable and adverse outcome groups, and predictive validity for adverse outcomes (N=21)



	Rutherford total injury score ≥ 7	NICHD $\geq 2A$
Sensitivity	83.3%	100%
Specificity	93.3%	73%
PPV	83.3%	60%
NPV	93.3%	100%
AUC	0.88	0.87

PPV=positive predictive value; NPV=negative predictive value; AUC=area under the curve

Figure 3: MRS metabolite ratios: comparing distributions of scores between favourable and adverse outcome groups, and predictive validity for adverse outcomes (N=19)



	Lactate:NAA ≥ 0.15	NAA:Creatine ≤ 1.34	NAA:Choline ≤ 2.46
Sensitivity	83.3%	83.3%	83.3%
Specificity	92.3%	92.3%	84.6%
PPV	83.3%	83.3%	71.4%
NPV	92.3%	92.3%	91.7%
AUC	0.88	0.88	0.84

PPV=positive predictive value; NPV=negative predictive value; AUC=area under the curve

specificity of Lac/NAA ≥ 0.15 for adverse outcome were 83% and 92%, respectively (AUC 0.88) (Figure 3).

CONCLUSION: We found neonatal MRI/MRS to be feasible in this Ugandan research population. The majority had evidence of hypoxia-ischaemia on MRI. Patterns of brain injury and Lac/NAA ratios differed from UK cohorts, reflecting high early mortality or differences in exposures and aetiology in this resource-limited care context. MRI and MRS were predictive of 18-month neurodevelopmental outcomes and could be utilised in future trials of novel neuroprotective strategies.

BIBLIOGRAPHY:

1. UN. Levels and Trends in Child Mortality Report 2020.
2. van Laerhoven. Pediatrics. 2013;131(1):88-98.
3. Nanyunja. Gates Open Res. 2022,6:10
4. Rutherford, Lancet Neurol. 2010;9(1):39-45.
5. Shankaran. NEJM. 2012;366(22):2085-92.

Comparison of clinical and brain MRI findings between Canadian and Dutch moderate-late preterm infant cohorts

Regan King¹, Emma Hofland-Burry¹, Gerda Meijler², Vivianne Boswinkel², Jeanne Scotland², Martijn F. Boomsma², Hussein Zein¹, Leonora Hendson¹, Khorshid Mohammed¹, Lara M. Leijser¹

¹University of Calgary, ²Isala Hospital

BACKGROUND: Approximately 12.5 million infants worldwide are born moderate to late preterm (MLPT) at 32-36 weeks' gestation each year. While at risk for brain lesions and neurodevelopmental problems, MLPT infants mostly do not qualify for the neurological surveillance (e.g., cranial ultrasound, developmental follow-up) routinely provided to very preterm infants (<32 weeks), resulting in often late diagnosis of problems (1). As recently shown by our team, clinical care guidelines for MLPT infants are limited and, if present, vary across neonatal centers (2). A better understanding of population characteristics and short- and long-term outcomes may enable advances in care and outcomes of MLPT infants. Our objectives were to study the occurrence of neonatal morbidity and brain lesions in a large cohort of MLPT infants born in Canada and The Netherlands, and compare occurrences between Canadian and Dutch infants.

METHODOLOGY: As part of the Brain Imaging in Moderate-late Preterm Infants (BIMP) study, brain Magnetic Resonance Imaging (MRI) around term-equivalent age (40-44 weeks PMA) was performed in 121 Canadian and 127 Dutch MLPT infants. For all infants, perinatal and neonatal data, such as mode of delivery, sex, small for gestational age (GA), need for respiratory support, sepsis, feeding difficulties and age at discharge, were collected. Conventional brain MR images (T1, T2, susceptibility) were assessed by three experts for brain lesion types common in very preterm infants, including hemorrhages (intraventricular [IVH], cerebellar [CBH], punctate), white matter injury, cystic lesions, infarction and signs of atrophy (irregular ventricles, wide extracerebral spaces). Perinatal and neonatal characteristics and occurrence brain lesions were calculated for all infants combined and compared between the Canadian and Dutch cohort using appropriate statistical tests.

RESULTS: The infants (61% male) had a mean GA of 34.4 weeks and birthweight of 2234 grams. All were admitted to neonatal units, and most frequently showed respiratory distress requiring support (40%). No significant differences in perinatal and neonatal characteristics were present between the Canadian and Dutch cohort, except for Canadian infants more often requiring respiratory support (53% vs 30%) and caffeine (56% vs 21%) (both $P < 0.05$). The most frequently detected brain lesions in

overall cohort were signs of atrophy (28%), IVH (11%) and CBH (11%), with most lesions considered to be mild and no significant differences in occurrence between the two cohorts ($P > 0.05$).

CONCLUSION: Our study confirms that MLPT infants, regardless of continent of birth, frequently experience neonatal morbidities and brain lesions. Also, the study suggests a differing approach to respiratory management and/or an effect of altitude between continents. Large cohort studies on the association between morbidities and later adverse neurodevelopmental outcomes, and the underlying mechanisms, are needed to standardize and advance the clinical care and therewith potentially outcomes of MLPT infants globally.

Lack of association between neurodevelopmental outcomes and MRI and inflammatory cytokines in neonatal encephalopathy

Arun Bokde, Deirdre Sweetman, Saima Aslam, Megan Ni Bhroin, Lynne Kelly, Mary O'Dea, Tim Hurley, Marie Slevin, Angela Byrne, Gabrielle Colleran, Eleanor Molloy

¹Trinity College Dublin

BACKGROUND: The objective is to evaluate whether neurodevelopmental outcomes at two years of age in NE are predicted by MRI brain scores and inflammatory cytokines. The MRI brain scores were the Barkovich, NICHD NRN and Weeke scoring systems, the four inflammatory cytokines were granulocyte macrophage-colony stimulating factor (GM-CSF), erythropoietin (EPO), interleukins (IL-8), and Vascular Endothelial Growth Factor (VEGF) and neurodevelopmental outcome at two years of age was measured with the Bayley-III.

METHODOLOGY: The infants for this study were part of three programmes: MODE [1], NEBULA [2], and NEPTuNE [3]. Data obtained from infants in these cohorts were used for retrospective analysis in the present study. Ethical approval was granted by the Ethics Committee at National Maternity Hospital, Holles Street, Dublin. Informed consent for participation in study was granted by legal guardian after the study was explained to them. Infants with NE were included according to the criteria of Huang et al [4]. Neuroimaging was carried out on or before 14 days of life. Serial blood samples in the first week of life were evaluated for multiplex cytokines. Therapeutic hypothermia (TH) was administered according to the TOBY criteria [5], with infants treated for a duration of 72 hours. Statistical analyses included general linear model (GLM) to assess the association between inflammatory cytokines (EPO, GM-CSF, IL-8,

Variable	Group (n=70)
Gestational age (weeks)	40.28 (34.86-44.00)
Postmenstrual age (weeks)	41.27 (35.72-45.00)
Age at scan (days)	6.94 (2-12)
Birth weight (kg)	3.72 (2.30-5.86)
Male	48
Mode of delivery:	
LCSC	27
SVD	19
Inst.	23
	(1 N/A)
Apgar: 1 minute	2.46 (0-9)
5 minutes	3.89 (0-9)
10 minutes	5.32 (1-10)
Therapeutic hypothermia	59
Seizures	43
	(1 N/A)
Sarnat: 0=normal	2
1=mild	8
2=moderate	50
3=severe	10
Mortality	4
	(4 N/A)
Cord pH 1	7.10 (6.79-7.37)
Cord pH 2	7.14 (6.81-7.34)
Cord BE 1 (mmol/l)	-10.81 (-21.30-5.90)
Cord BE 2 (mmol/l)	-9.99 (-19.00-5.30)

Table 1. Neonatal demographic characteristics. Data presented as means (with range) or n (number of infants). Abbreviations: BE, base excess; Inst., instrumental delivery; LCSC, lower segment Caesarean section; SVD, spontaneous vaginal delivery.

VEGF) and MRI brain scores (Barkovich, NICHD NRN, Weeke, normal/abnormal MRI). This was performed separately for each cytokine and each scoring system. Log values for each cytokine were used for this analysis, in order to transform the data from skewed to normally distributed.

RESULTS: There were 70 infants included in analysis from the 136 recruited for the original studies – the 70 had complete MRI scores, inflammatory markers, and Bayless-III scores – see Table 1 and 2 for demographics and clinical scores, and MRI scores, respectively. No statistical association was detected between the independent factors MRI score and inflammatory markers (EPO, IL-8, VEGF) with outcome variable Bayless-III scores in GLM model. There was a trend to statistical significance (table 3) in the model that included GM-CSF as independent factor with all 3 MRI scoring systems.

CONCLUSION: It may be that the Weeke grey matter scoring system may be the most sensitive to inflammatory

Variable	Group (n=70)
Barkovich (BG/W):	
0	47
1	8
2	7
3	7
4	1
NICHD NRN:	
0	44
1A	3
1B	7
2A	7
2B	8
3	1
Weeke:	
Grey matter	2.69 (0-23)
White matter	3.20 (0-17)
Cerebellum	1.76 (0-4)
Total overall score	8.06 (0-45)
Normal/abnormal MRI:	
Normal	47
Abnormal	23

Table 2. Neonatal MRI scoring characteristics. Data presented as means (with range) or n (number of infants). Abbreviations: BG/W, basal ganglia/watershed; MRI, magnetic resonance imaging; NICHD NRN, National Institute of Child Health and Human Development Neonatal Research Network.

Scoring System	FDR corrected p-value for GM-CSF and cognitive scores
Barkovich BG/W	0.077
NICHD NRN	0.058
Weeke Grey Matter	0.067
Weeke White Matter	0.133
Weeke Cerebellum	0.050
Weeke Overall	0.053
Normal/Abnormal MRI (Barkovich)	0.058

Table 3. FDR corrected p-values for GM-CSF combined with each MRI scoring system, and cognitive outcome scores. Abbreviations: BG/W, basal ganglia/watershed; FDR, false discovery rate; GM-CSF, Granulocyte Macrophage-Colony Stimulating Factor; MRI, magnetic resonance imaging; NICHD NRN, National Institute of Child Health and Human Development Neonatal Research Network.

markers in NE in a model to predict outcome. Further studies with larger sample sizes are needed.

REFERENCES

[1] Sweetman D. 2014. PhD thesis, Royal College of Surgeons in Ireland.
 [2] Aslam S. 2017. PhD thesis, Royal College of Surgeons in Ireland.
 [3] Molloy EJ et al. HRB Open Res. 2020;3(40):40.
 [4] Huang CC et al. N Engl J Med. 1999 ;341(5):328-35.
 [5] Azzopardi DV et al. N Engl J Med. 2009 Oct 1;361(14):1349-58.

Do measurements matter?: Impact of 2d lateral ventricular size on outcome in preterm infants

Raphaella Jernej¹, Renate Fuiko¹, Gregor Kasprian², Angelika Berger¹, Katharina Goeral¹

¹Medical University of Vienna, Comprehensive Center for Pediatrics, Department of Pediatrics and Adolescent Medicine, Division of Neonatology, Intensive Care and Neuropediatrics, ²Medical University of Vienna, Department of Radiology, Division of Neuroradiology and Musculoskeletal Radiology

BACKGROUND: Bedside cranial ultrasound (cUS) is cost-effective, widely available, and is performed routinely on a daily basis. Studies showed a correlation between anterior horn width (AHW) measured in 2D ultrasound and neurodevelopmental outcome in infants with PHVD, but little is known about the role of ventricular index (VI), AHW and thalamo-occipital distance (TOD) in preterm neonates.

METHODOLOGY: Retrospective, single-center study of serial cUS scans in preterm neonates born <32 weeks

applying 2D measurement techniques (VI, AHW, TOD). A composite score was calculated using the median for a certain gestational age as a cutoff for the maximum value of every parameter and patient (maximum score of 3). Our aim was to investigate the impact of the mentioned parameters on neurodevelopmental outcome at 12 months corrected age.

RESULTS: A total of 79 serial cUS scans in a cohort of 32 patients were available for analysis. Median GA at birth was 25 weeks and 35 weeks at scan. In 80% of scans, all measured parameters were <97th percentile. Median composite score was 1 (IQR 0-2). Median outcome scores were 96 for cognition, 90 for language and 95 for motor development. Considering every single parameter, as well as the composite score, there was no significant impact on specific outcome domains. Regarding outcome categories, a significant impact of our composite score on motor outcome ($p=0.042$) was observed.

CONCLUSION: There was no significant impact of ventricular measurements in serial cranial ultrasound on neurodevelopmental outcome at 12 months corrected age. However, using a composite score for each patient a significant impact on motor outcome categories was found. Data with a higher number of patients is in progress and will be available until the conference (aim = 200 patients).